2012-01-01

Constrained Optimal Control For A Multi-Group Discrete Time Influenza Model

Paula Andrea Gonzalez Parra
University of Texas at El Paso, paulag817@gmail.com

CONSTRAINED OPTIMAL CONTROL FOR A MULTI-GROUP

DISCRETE TIME INFLUENZA MODEL

PAULA A. GONZALEZ PARRA, MSc

Program in Computational Science

APPROVED:

Martine Ceberio, Chair, Ph.D.

Carlos Castillo-Chavez, Co-Chair, Ph.D.

Sara Del Valle, Ph.D.

Vladik Kreinovich, Ph.D.

Benjamin C. Flores, Ph.D.
Dean of the Graduate School

To my family and

to the memory

of my lovely aunt Blanca Ines,

she was always my support and motivation.

CONSTRAINED OPTIMAL CONTROL FOR A MULTI-GROUP *DISCRETE TIME INFLUENZA MODEL*

by

PAULA A. GONZALEZ PARRA, MSc

THESIS

Presented to the Faculty of the Graduate School of

The University of Texas at El Paso

in Partial Fulfillment

of the Requirements

for the Degree of

DOCTOR OF PHILOSOPHY

Program in Computational Science

THE UNIVERSITY OF TEXAS AT EL PASO

December 2012

Acknowledgements

I would like to express my deeply gratitude to my advisor, Dr. Martine Ceberio from the Computer Science Department at The University of Texas at El Paso, for her incredible support and advice. She is a great role model, advisor and teacher.

I also wish to thank my coadvisor Dr. Carlos Castillo-Chavez. He has been a great influence in my life. He gave me the opportunity to attend the Mathematical and Biology Theoretical Institute, MTBI at Arizona State University every summer from 2009 to 2012. It was a great experience for both my academic and personal life. I want to thanks all the people involve with MTBI, specially to Dr. Sunmi Lee who was my mentor and friend, and Dr. Karen Rios-Soto, my lovely friend who made my life happier every summer.

Special thanks to my committee members Dr. Sara Del Valle and Dr. Vladick Kreinovich for their comments, sugestions and support.

Additionally, I want to thank The University of Texas at El Paso and the Computational Science Program, in particular, Dr. Miguel Argaez and Dr. Leticia Velazquez who gave me the opportunity to start my Ph.D at UTEP. I also want to thanks the Puentes Program and the Writing Center at UTEP.

Thanks to the American Association for University Women, because of their financial support I finished my dissertation sooner. Thanks to the Pan American Round Table of Texas and the Cotton Scholarship from the University of Texas at El Paso. All my gratitude to the Universidad Autonoma de Occidente, Cali-Colombia.

My family have been a incredible support, I thank my mother Isabel, my father Arturo, my brother Andres, his wife Sandra, and my future nephew Alejandro who is giving me a lot of inspiration and motivation. I extend my gratitude to all my family, aunts, uncles and cousins for their support.

Thanks God for all the good people that make my life nicer during my time as a Ph.D student, specially my Colombian family in el Paso, Rei, Mirel, Carlos, Julio, padre Wilson,

and padre Mena.

Finally, I must thank my dear loving support, Anibal Sosa, he has been a great motivation, he gives me a lot of reasons to smile every day. Thanks for being with me not only in good times but also in hard ones.

NOTE: This thesis was submitted to my Supervising Committee on the Nov 26, 2012.

Abstract

During the last decades, mathematical epidemiological models have been used to understand the dynamics of infectious diseases and guide public health policy. In particular, several continuous models have been considered to study single influenza outbreaks and the impact of different control policies. In this dissertation, a discrete time model is introduced in order to study optimal control strategies for influenza transmission; since epidemiological data is collected on discrete units of time, a discrete formulation is more efficient. From a mathematical point of view, continuous time model are easier to analyze, however, the numerical solution of discrete-time models is simpler and therefore can be easily implemented.

We formulated a discrete susceptible-infected-treated-recovered (SITR) model. We evaluated the potential effect of control measures, such as social distancing and antiviral treatment in the context of a single influenza outbreak. The objective was to minimize the total number of infected individuals at the end of the epidemic in a most economical way. The potential effect of antiviral treatment was evaluated by considering both unlimited and limited supply. We found that the use of single and dual strategies (social distancing and antiviral treatment) resulted in reductions in the cumulative number of infected individuals. In the case of limited resources, our results showed that in order to control the epidemic, most of the resources must be utilized at the beginning of the epidemic until all the resources exhausted.

The optimal control problem was solved by using two different techniques: 1) By using a discrete version of Pontryagin's maximum principle, with the commonly used forward-backward algorithm; and 2) by using the primal-dual interior-point method. The later approach allowed the inclusion of constraints more efficiently and solved the problem in fewer iterations. The main advantage of interior-point methods was that constraints can be included in a simple way; in particular, the isoperimetric constraint in the case of limited resources. However, since this technique is based on the Newton Method, the solution was very sensitive to initial conditions.

In addition, the role of heterogeneity in the population was considered. The total population was divided into subgroups according to activity or susceptibility levels. The goal was to determine how treatment doses should be distributed and how social distancing should be implemented in each group in order to reduce the final epidemic size. We presented numerical results for two and three groups, both for the case of seasonal and pandemic influenza. The results were sensitive to different population sizes; that is, our results showed that in order to control an epidemic, more resources need to be channeled towards the group with the largest population and most active.

Finally, we considered another optimization problem derived for the same epidemiological model in which, instead of minimizing the number of infected individuals, we estimated parameter values from historical epidemic data in order to identify features, such as contact rate and recovery rate. Although the parameter values used in the model were estimated from epidemiological data, there is still some uncertainty in their values. Thus, we introduced some basic ideas and examples of parameter estimation applied to discrete epidemiological models. Our goal was to present all the tools necessary to better estimate parameter values and implementation of optimal control measures. We found that a discrete formulation allows us to solve the parameter estimation problem in a simpler way.

Table of Contents

List of Tables

List of Figures

Chapter 1

Introduction

In April of 2009, the World Health Organization (WHO) announced the emergence of a novel influenza A (H1N1) [21]. National and international public health agencies quickly took (often drastic) emergency measures to contain the spread of the virus; however, in June of 2009, the WHO declared novel influenza A (H1N1) a pandemic.

During the last few decades, mathematical epidemiological models have been used to understand infectious disease dynamics and provide public health policy guidance [3, 29]. In particular, continuous time models have been used to study influenza outbreaks and the impact of different control policies [7, 22, 31, 46, 51]. Optimal control models have been used to evaluate the impact of control strategies for many applications [10, 42, 47] including antiviral treatment and the isolation of infectious individuals [39, 40, 50]. Traditionally, epidemiological models use continuous-time dynamics [17, 22, 23, 24, 27] because they are more tractable from the mathematical point of view. However, more recently, there has been an increased interest in the use of discrete transmission models [1, 2, 13, 15, 16]; a good reason for using discrete models is because data is collected in time intervals (i.e., discrete time).

In our work, we introduce a novel discrete time influenza model following the approaches in [15, 16], and formulate a discrete optimal control problem in order to evaluate the effects of social distancing and antiviral treatment as control measures. The objective is to minimize the total number of infected individuals at the end of the epidemic in the most economical way. The optimal control problem is solved by using two different methodologies: a discrete version of the well-known Pontryagin's maximum principle and primal-dual interior-point methods. The Pontryagin's maximum principle in general is applied by using

the backward-forward algorithm [28, 39, 40, 42] and it has many applications, in particular to epidemiological problems [25, 34, 37, 38, 39, 40, 42]. On the other hand, to the best of our knowledge, interior-point methods have not been previously used to solve control problems in epidemiology. The main advantage of using this approach is that it allows us to include explicit lower and upper bounds in the formulation.

We present the formulation of the optimal control problem and both methods in Chapter 3. One of the main contributions of this dissertation is the formulation of the optimal control problem as a non-linear programming problem and its solution by using interior-point methods. The solution, for both methods, is presented in Chapter 3. In addition, we compare three different strategies: social distancing, treatment, and a combination of both mitigation strategies under different scenarios. The impact of each strategy is considered in terms of the reduction of the final epidemic size, i.e, the total number of infected individuals at the end of the epidemic.

Since the dynamics of many diseases such as measles and influenza are strongly correlated with age [17], in Chapter 4, we generalize our model in order to study the role of heterogeneity. We formulate a discrete group-structured influenza model by divided the population into subgroups according to susceptibility or activity levels. Previous research on influenza models, including group structure, have been done in the continuous case. Numerical simulations for two and three subgroups are presented for different scenarios for both seasonal and pandemic influenza.

In Chapters 3 and 4, we have considered the ideal case of unlimited resources. In Chapter 5, we present a more realistic scenario by assuming that treatment doses are limited. In this case we include an isoperimetric constraint [40, 42]. A similar problem was considered in [40] for a continuous time influenza model by using Pontryagin's maximum principle. The authors remarked that convergence issues have to be addressed. Our results shows that primal-dual interior-point method allows the inclusion of the isoperimetric constraint in a simple way.

Finally, we present a different optimization problem. Since epidemiological models con-

tain parameters, in order to compare the model predictions with real data, the parameter values should be estimated. In Chapter 6, we present some basic ideas and examples of parameter estimation applied to discrete epidemiological models. Two techniques are presented: Ordinary Least Squares and Generalized Least Squares. Following the ideas from [9], we estimate some parameters of a discrete SITR model by using synthetic data. We also use data sets from an influenza outbreak in a border school in the United Kingdom and from the 1918 influenza pandemic in San Francisco.

Chapter 2

Problem Formulation

In this chapter we present the core epidemiological model that we will study in this dissertation. We present the basic epidemiological assumptions and the control measures that we want to consider in order the reduce the number of infected individuals at the end of the epidemic. In addition, we introduce the control policies that we consider and we formulate the core optimal control problem.

2.1 Epidemiological Model

One of the most important contribution in mathematical epidemiology was the formulation of a simple compartmental model by Kermack and McKendrick in 1927 [11, 36]; which use a continuous model based on assumptions on the rates of flow of individuals between different classes. Traditionally, epidemiological models have used continuous-time dynamics [12] because they are more tractable from the mathematical point of view. Most recently, there has been an increased interest in the use of discrete disease transmission models [1, 2, 13, 15, 16], however, to our knowledge, there are limited studies that have used discrete epidemic models [37, 38, 55]. The use of discrete models is attractive because experimental data is typically collected in time intervals (i.e, discrete time).

We formulate a discrete time Susceptible-Infectious-Recovered (SIR) model following the approaches introduced in [15, 16], where the total population (N) is divided into three classes: Susceptible (S), Infectious (I), and Recovered (R) individuals. Since we consider a single outbreak, births and deaths from natural causes are ignored ($N = S + I + R$). We use the subindex t to denote the number of individuals of each class at time t, and the range

of $t \in [0, n]$, where n denotes the final time of a single epidemic outbreak. The fraction of susceptible individuals at time t that get infected at time $t+1$ is modeled by the function

$$G_t = \rho \frac{I_t}{N_t},$$

where ρ is the susceptibility rate. The proportion of disease-induced deaths per generation is denoted by δ. It is assumed that infectious individuals *naturally* recover with probability σ_1 (per generation). In Figure 2.1, we present a flow diagram of the disease dynamics for the SIR model without any control. In this diagram, every compartment represents a class of individuals; people move from one compartment to other as they change epidemic status, they can move either from Susceptible to Infected or from Infected to Recovered. Some of the infected individuals can be removed from the population because of the disease induced death.

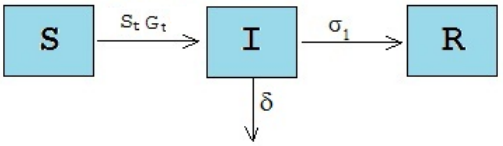

Figure 2.1: Compartmental flow diagram for the SIR model. Individuals move from one compartment to other when they change epidemic status. Some of the infected individuals are removed from the population because of the disease induced death.

The model (without control) is given by the following system of nonlinear difference equations:

$$\begin{aligned} S_{t+1} &= S_t(1 - G_t) \\ I_{t+1} &= S_t G_t + (1 - \sigma_1)(1 - \delta) I_t \\ R_{t+1} &= R_t + \sigma_1 (1 - \delta) I_t. \end{aligned} \tag{2.1}$$

We calculate the basic reproductive number R_0 by using the next generation operator approach described in [2]. In epidemiology, R_0 is defined as the number of secondary cases produced by a single infected individual in a population of susceptible individuals. For the

SIR Model (2.1) R_0 is given by:

$$R_0 = \frac{\rho}{1-(1-\sigma_1)(1-\delta)}. \tag{2.2}$$

Notice that ρ is the susceptibility rate and $\frac{1}{1-(1-\sigma_1)(1-\delta)}$ is the expected time in the infectious period. In the next sesion, we introduce a model that includes control policies such as social distancing and antiviral treatment. Our goal is to study the impact of different control policies in reducing disease spread.

2.2 Optimal Control Problem

Optimal control theory is a powerful mathematical tool than can be used to make decisions involving real life situations. For example, for a given epidemic, we are interested in the percentage of the population that should be treated in order to minimize the number of infected individuals and the cost of treatment implementation. In this section, we present an optimization formulation that is called "an optimal control problem." These problems were introduced in the 1950s, motivated especially by aerospace applications [28]. The main idea is to find an optimal control solution for a system, that is described by differential or difference equations. The behavior of the dynamical system is described by the **state** variables, and we assume that there is a way to manage the state by using some **control functions**. The goal is to find a control that minimizes a given **objective functional**. The control that minimize the objective functional will be called an **optimal control solution**.

Pontriagyn, Boltyanskii, and Gamkrelidze found the necessary conditions for finding an optimal solution [28] of this problem; these optimality conditions are known as the Pontryagin's Maximum Principle. Hence, the system of difference equations (2.1) is modified in order to introduce social distancing and antiviral treatment as control variables. The goal is to reduce the number of infected individuals by using the least amount of resources from social distancing and antiviral treatment.

We modify Model (2.1) and introduce the new model. We consider that the fraction of infected individuals who are treated at each generation t is modeled by the *antiviral treatment*

control function labeled as τ_t. The *social distancing control* function, denoted by x_t, models the reduction in the number of contacts per unit of time. In our case the unit of time is days, for example is $x_{30} = .1$, each individual should reduce the number of contacts by 10% in the day 30. Figure 2.2 shows the disease dynamics of the Susceptible-Infected-Treated-Recovered (SITR) model with controls. This diagram is a modification of Figure 2.1, the class of treated individuals is introduced, individuals from the Infected class can move either to Treated or Recovered class.

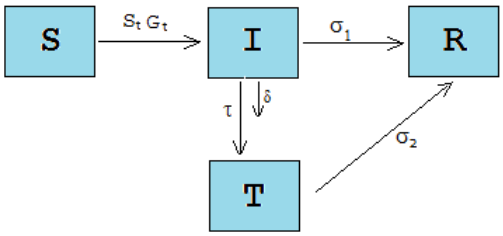

Figure 2.2: Compartmental flow diagram for the control SITR model.

Since treated individuals are still infectious, the fraction of susceptible individuals at time t that remain susceptible at time $t+1$ is modeled by the function:

$$G_t = \rho(1 - x_t)\frac{I_t + \epsilon T_t}{N_t}, \tag{2.3}$$

where ϵ represents the effectiveness of the treatment $(0 < \epsilon \leq 1)$. The model is then given by the following modified system of difference equations:

$$\begin{aligned} S_{t+1} &= S_t(1 - G_t) \\ I_{t+1} &= S_t G_t + (1 - \tau_t)(1 - \sigma_1)(1 - \delta) I_t \\ T_{t+1} &= (1 - \sigma_2) T_t + \tau_t (1 - \sigma_1)(1 - \delta) I_t \\ R_{t+1} &= R_t + \sigma_1 (1 - \delta) I_t + \sigma_2 T_t. \end{aligned} \tag{2.4}$$

Our goal is to minimize the number of infected individuals over a finite time interval $[0, n]$ by using the least amount of treatment and social distancing. Therefore, we pose the

constrained optimal control problem as:

$$\begin{aligned} &\text{minimize } \frac{1}{2}\sum_{t=0}^{n-1}\left(B_1 I_t^2 + B_2 x_t^2 + B_3 \tau_t^2\right) \\ &\text{subject to Model 2.4,} \\ &\qquad 0 \le x_t \le x_{\max}, \\ &\qquad 0 \le \tau_t \le \tau_{\max}. \end{aligned} \tag{2.5}$$

where $x_{\max}$ and $\tau_{\max}$ are upper bounds that represent the maximum allowed values for each control per unit of time. The weight constants B_1 to B_3 are a measure of the *relative* cost of interventions over $[0, n]$. In particular, B_2 and B_3 denote the relative costs associated with the implementation of social distancing and antiviral treatment, respectively. Although we do not know the real cost of each of these strategies, constants B_i's allow us to make assumptions on their relative costs: for instance when B_2 is greater than B_3, it means that we assume that the implementation of social distancing will be more costly than that of antiviral treatment. We will set the weight constants values in part to facilitate computational issues and according to the scenario that we want to consider. Note however that the model as we designed it is robust to different values of B_i's; as a result, although for the purpose of this work, we set the B_i's to specific values, our model could handle other values and therefore account for different and more strategies. We evaluate the *relative* impact of each of the following control strategies applied to model (2.5):

Strategy 1: Social distancing ($x_t \ge 0$, $\tau_t = 0$),

Strategy 2: Antiviral treatment ($\tau_t \ge 0$, $x_t = 0$),

Strategy 3: Both social distancing and antiviral treatment ($x_t \ge 0$, $\tau_t \ge 0$).

The relative impact of each strategy is evaluated and compared on the final epidemic size, i.e., on the number of infected individuals at the end of the epidemic, under single or dual policies. Notice that each strategy will represent a different optimization problem. The final

time n is a value between 180 and 250 days; we choose this value by running simulations without control, n is the number of days that the epidemic remains in the population. This value depends of the basic reproductive number R_0. For a small value of R_0, we have a big value of n, because the epidemic will take longer to spread over the population.

Summary of contribution: the formulation of a novel discrete time influenza model, following the approach in [15, 16], is the main contribution of this chapter. By using the next generation operator [2], we calculated the basic reproductive number R_0, that is, the number of secondary cases produced by a single infected individual in a population of susceptible individuals. We introduced treatment and social distancing as control policies and we formulated a core optimal control problem, this problem will be modified for each strategy.

In the next chapter, each particular optimization problem is solved using two different methodologies: the well-known discrete version of Pontryagin's maximum principle [32, 33, 42] and primal-dual interior-point Method [5, 6, 45, 26, 54]. The first method has been widely used to solve optimal control problems in epidemiology [25, 34, 39, 40]. The second technique has been applied successfully in different areas, but to our knowledge, there is little evidence of its applications within epidemiological problems. We present both methodologies in the next chapter and numerical results by considering different strategies and scenarios.

Chapter 3

Solution of the Simple Optimal Control Problem

In this chapter, we present two methodologies for solving the constrained optimal control problem (2.5): the Pontryagin's maximum principle and the primal-dual interior-point method. There are many applications of the first methodology to optimal control problems in epidemiology [37, 39, 40] but as far as we know there is not evidence of interior-point methods applied to epidemiological problems. One of the main contributions of this dissertation is the formulation of problem (2.5) as a nonlinear programming problem and the use of interior-point methods to solve it. We present numerical results by solving the simple problem (2.5) presented in the previous chapter using both methodologies and different scenarios. For example, we consider different control strategies, different values of the basic reproductive number R_0, and different weight constants.

3.1 Pontryagin's Maximum Principle

Pontryagin's maximum principle is a classical result of control theory that provides the necessary conditions for finding an optimal solution. Since our focus is to solve a discrete optimal control problem, we use a discrete version of Pontryagin's maximum principle [32, 33, 42].

The control and state variables are denoted by $\mathbf{u} = (u_0, u_1, \ldots, u_{n-1})$ and $\mathbf{x} = (x_0, x_1, \ldots, x_n)$, respectively. The subindex represents the time step $t = 0, 1, \ldots, n$. The state equation for a

given initial condition x_0, is given by the difference equation:

$$x_{t+1} = g(x_t, u_t, t). \tag{3.1}$$

The objective functional is defined by:

$$J(\mathbf{u}) = \Phi(x_n) + \sum_{t=0}^{n-1} f(x_t, u_t, t),$$

where f, g, and Φ are continuously differentiable functions; therefore, the constrained problem is:

$$\begin{aligned} &\text{minimize} \quad J(\mathbf{u}) \\ &\text{subject to} \quad \text{Model (3.1)}. \end{aligned}$$

We introduce the adjoint variable λ_t and define the Hamiltonian at time t as

$$H_t = f(x_t, u_t, t) + \lambda_{t+1} g(x_t, u_t, t), \text{for } t = 0, 1, \ldots, n-1.$$

The necessary conditions as described in [42] are given by:

1. The adjoint equation
$$\lambda_t = \frac{\partial H_t}{\partial x_t}, \tag{3.2}$$

2. The transversality condition at the state solution x_n^*
$$\lambda_n = \Phi'(x_n^*), \tag{3.3}$$

3. The optimality condition at the optimal solution u^*
$$\frac{\partial H_t}{\partial u_t} = 0.$$

These three conditions are similar to the ones in the continuous case, the only difference is that we do not have a negative sign in the adjoint equation (3.2). Usually in biological applications, the numerical solution is found by using the Forward-Backward algorithm [4, 42, 37, 39]. This algorithm can be used for both the discrete and continuous cases.

3.1.1 Forward-Backward Method

In this section, we apply the Forward-Backward algorithm [4, 42, 37, 39] to our particular problem. We denote the control variables as $\mathbf{x} = (x_0, x_1, \ldots, x_{n-1})$ and $\boldsymbol{\tau} = (\tau_0, \tau_1, \ldots, \tau_{n-1})$ representing social distancing and treatment, respectively. Let $\mathbf{y}_t = (S_t, I_t, T_t, R_t)^T$ be the state variable with $t = 0, 1, \ldots, n$, and the objective functional:

$$\mathcal{F}(\mathbf{x}, \boldsymbol{\tau}) = \frac{1}{2} \sum_{t=0}^{n-1} F(\mathbf{y}_t, x_t, \tau_t, t),$$

where:

$$F(\mathbf{y}_t, x_t, \tau_t, t) = B_1 I_t^2 + B_2 x_t^2 + B_3 \tau_t^2. \tag{3.4}$$

The weight constants B_1 to B_3 are a measure of the *relative* cost of interventions over $[0, n]$. In particular, B_2 and B_3 denote the relative costs associated with the implementation of social distancing and antiviral treatment, respectively. The use of these notations and definitions leads to the problem of finding discrete control functions $\mathbf{x}$ and $\boldsymbol{\tau}$ such that:

$$\begin{aligned} &\underset{U}{\text{minimize}} \quad \mathcal{F}(\mathbf{x}, \boldsymbol{\tau}) \\ &\text{subject to} \quad \text{Model (3.6)}, \end{aligned} \tag{3.5}$$

where $U = \{(x_t, \tau_t) : 0 \leq x_t \leq x_{\max}, 0 \leq \tau_t \leq \tau_{\max}, t = 0, 1, \ldots, n-1\}$ and Model (3.6) is the model introduced in Chapter 2, that is:

$$\begin{aligned} S_{t+1} &= S_t(1 - G_t) \\ I_{t+1} &= S_t G_t + (1 - \tau_t)(1 - \sigma_1)(1 - \delta) I_t \\ T_{t+1} &= (1 - \sigma_2) T_t + \tau_t (1 - \sigma_1)(1 - \delta) I_t \\ R_{t+1} &= R_t + \sigma_1 (1 - \delta) I_t + \sigma_2 T_t. \end{aligned} \tag{3.6}$$

The Hamiltonian associated with Problem (3.5) is given by:

$$H_t = F(\mathbf{y}_t, x_t, \tau_t, t) + \boldsymbol{\lambda}_{t+1}^T \mathbf{y}_{t+1},$$

where x_t, τ_t are the control variables, $\mathbf{y}_t, \boldsymbol{\lambda}_t \in \mathbb{R}^4$ are the state and adjoint variables respectively. The adjoint equations are:

$$\lambda_t^i = \frac{\partial H_t}{\partial y_t^i}, \quad \text{with} \quad i = 1, 2, 3, 4, \tag{3.7}$$

where λ_t^i and y_t^i are the i-th component of $\boldsymbol{\lambda}_t$ and $\mathbf{y}_t$, respectively. Finally, the optimality conditions are:

$$\frac{\partial H_t}{\partial x_t} = 0 \text{ and } \frac{\partial H_t}{\partial \tau_t} = 0.$$

The procedure to find optimal solutions is summarized in Algorithm 1 [4, 42].

Algorithm 1 Forward-Backward Algorithm

1: Initial values for $\mathbf{x}$, $\boldsymbol{\tau}$ and condition $\mathbf{y}_0$ are selected.

2: **for** $k = 0, 1, 2 \ldots$ until convergence **do**

3: Solve the state equation (2.4) forward in time.

4: Solve the adjoint equation (3.7) backward in time; subject to the transversality conditions $\boldsymbol{\lambda}_n = 0$, where n is the final time.

5: Solve the optimality conditions:

$$\frac{\partial H_t}{\partial x_t} = 0 \text{ and } \frac{\partial H_t}{\partial \tau_t} = 0.$$

6: Check convergence:

$$\text{if } \frac{\|\mathbf{u} - \mathbf{u}_{old}\|}{\|\mathbf{u}\|} < 0.001, \text{for } \mathbf{u} \in \{\mathbf{x}, \boldsymbol{\tau}\}, \text{ break}$$

7: **end for**

3.2 Primal-Dual Interior-Point Method

Interior-Point Methods (IPM) were introduced by Karmarkar in 1984 [35] for solving linear programming problems and his seminal work has been extended for solving large scale nonlinear programming problems (e.g., Problem (3.5)). Contrary to the simplex method, which finds an optimal solution by testing the adjacent vertices of a feasible set, IPM find optimal solutions by crossing the interior of a feasible region. Figure 3.1 shows a geometrical interpretation of IPM in the case of linear programming, when the solution set is an edge including the vertices.

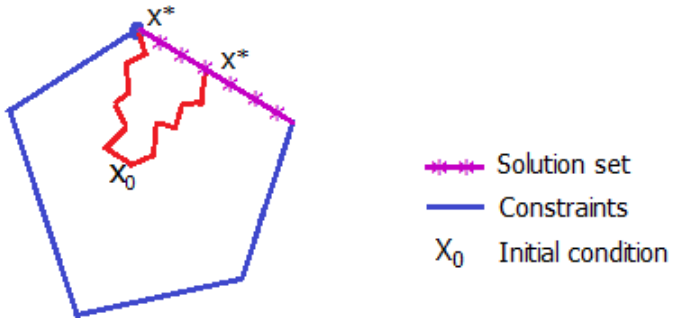

Figure 3.1: Geometrical interpretation of IPM in the case of linear programming. Each edge represents the frontier of a linear constraint, the line with stars is the solution set.

The simplex method is shown to have exponential complexity, because it may go through almost all the corners before finding a solution. Computationally, IPM are more efficient than the simplex method because they have polynomial complexity. In addition, the simplex method finds solutions at the corner points only, while IPM may find solutions in the interior as well. Before introducing the interior-point methodology, we present some terminology and definitions.

A general nonlinear programming problem is given by:

$$\begin{aligned} \text{minimize} \quad & f(x) \\ \text{subject to} \quad & h(x) = 0, \\ & x \geq 0, \end{aligned} \tag{3.8}$$

where $f : \mathbb{R}^n \to \mathbb{R}$ and $h : \mathbb{R}^n \to \mathbb{R}^m$. The Lagrangian function associated with Problem (3.8) is defined as:

$$L(x, y, z) = f(x) + h(x)^T y - x^T z.$$

The Karush-Kuhn-Tucker (KKT) conditions are the necessary conditions for a solution of a nonlinear programming problem to be optimal [45]. For Problem (3.8), the KKT conditions

are given by:

$$F(x,y,z) = \begin{bmatrix} \nabla_x L(x,y,z) \\ h(x) \\ XZe \end{bmatrix} = 0,$$

where $F : \mathbb{R}^{n+m+n} \to \mathbb{R}^{n+m+n}$, $\nabla_x L(x,y,z) = \nabla_x f + \nabla h(x)^T y - z$, $X = diag(x)$, $Z = diag(z)$, and $e = (1, \ldots, 1) \in \mathbb{R}^n$.

Now we introduce the perturbed KKT conditions [45, 26] associated with Problem (3.8):

$$F_\mu(x,y,z) = \begin{bmatrix} \nabla_x L(x,y,z) \\ h(x) \\ XZe - \mu e \end{bmatrix} = 0, \tag{3.9}$$

where $F_\mu : \mathbb{R}^{n+m+n} \to \mathbb{R}^{n+m+n}$ and $\mu \geq 0$. Notice that the perturbation is made just in the last equation, known as the *complementarity condition*, in order to avoid "sticking to the boundary" before reaching a solution. The term "sticking to the boundary" refers to when an x_i or z_i becomes zero before reaching a solution, subsequently x_i^+ will be zero, i.e., if $x_i = 0$ and $z_i \neq 0$ then $\Delta x_i = 0$ and $x_i^+ = x_i + \Delta x_i = 0$, hence the algorithm will diverge. We use Newton's method to solve (3.9); therefore, the Jacobian associated with (3.9) is:

$$F'(x,y,z) = \begin{bmatrix} \nabla_x^2 L & \nabla h(x)^T & I_{n\times n} \\ \nabla h(x) & 0_{m\times m} & 0_{m\times n} \\ Z & 0_{n\times m} & X \end{bmatrix},$$

the Newton system associated with (3.9) is given by:

$$F'(x,y,z)\Delta s = -F_\mu(x,y,z), \tag{3.10}$$

where $\Delta s = [\Delta x, \Delta y, \Delta z]^T$.

3.2.1 Primal-Dual Interior-Point Method for The Optimal Control Problem

One of the main contributions of this dissertation is the formulation of the optimal control problem (2.5) as a nonlinear programming problem:

$$\begin{aligned} \text{minimize} \quad & f(y) \\ \text{subject to} \quad & E(y) = 0, \\ & 0 \leq y \leq y_{\max}, \end{aligned} \tag{3.11}$$

where $\mathbf{y} = (S_1, I_1, T_1, x_0, \tau_0, \ldots, S_n, I_n, T_n, x_{n-1}, \tau_{n-1})^T$ and n is the final time. The objective functional is given by $f : \mathbb{R}^{5n} \to \mathbb{R}$, where:

$$f(y) = \frac{1}{2}\left(B_1\|\tilde{I}\|^2 + B_2\|x\|^2 + B_3\|\tau\|^2\right), \tag{3.12}$$

with $\tilde{I} = (I_0, I_1, \ldots, I_{n-1})^T$, $x = (x_0, x_1, \ldots, x_{n-1})^T$, and $\tau = (\tau_0, \tau_1, \ldots, \tau_{n-1})^T$.

From Model (2.4), we get the equality constraint $E : \mathbb{R}^{5n} \to \mathbb{R}^{3n}$,

$$E(y) = \begin{pmatrix} S_1 - S_0(1 - G_0) \\ I_1 - S_0G_0 - (1 - \tau_0)(1 - \sigma_1) I_0 \\ T_1 - (1 - \sigma_2) T_0 - \tau_0 (1 - \sigma_1) I_0 \\ \vdots \\ S_n - S_{n-1}(1 - G_{n-1}) \\ I_n - S_{n-1}G_{n-1} - (1 - \tau_{n-1})(1 - \sigma_1) I_{n-1} \\ T_n - (1 - \sigma_2) T_{n-1} - \tau_{n-1} (1 - \sigma_1) I_{n-1} \end{pmatrix} = 0, \tag{3.13}$$

where G_i is given in (2.3). We consider just S, I, and T because R does not participate in the disease dynamics. Finally, the inequality constraint $y \leq y_{\max}$ can be written as $y_{\max} - y \geq 0$. This constraint represents the upper bounds for the controls u and τ, which are interpreted as the maximum daily rates.

Now we describe the primal-dual interior-point methodology used to solve problem (3.11). Following the ideas presented in Section 3.2, the Lagrangian associated with (3.11) is given

by:

$$L(y, w, z) = f(y) + E(y)^T w - y^T z_1 - (y_{\max} - y)^T z_2,$$

where w, z_1, and z_2 are the Lagrange multipliers associated with the equality and inequality constraints, respectively. Therefore the perturbed KKT conditions are given by:

$$F_\mu(y, w, z_1, z_2) = \begin{bmatrix} \nabla_y L(y, w, z_1, z_2) \\ E(y) \\ Y Z_1 - \mu e \\ (Y_{\max} - Y) Z_2 - \mu e \end{bmatrix} = 0, \tag{3.14}$$

where:

$$\begin{aligned} F_\mu &: \mathbb{R}^{5n+3n+5n+5n} \to \mathbb{R}^{5n+3n+5n+5n}, \\ \nabla_y L &= \nabla_y f + \nabla E^T w - z_1 + z_2, \\ Y &= \operatorname{diag}(y), \\ Y_{\max} &= \operatorname{diag}(y_{\max}), \\ Z_1 &= \operatorname{diag}(z_1), \\ Z_2 &= \operatorname{diag}(z_2), \text{ and} \\ e &= (1, \ldots, 1) \in \mathbb{R}^{5n}. \end{aligned}$$

From (3.9) and (3.10), the Newton system associated with problem (3.11) is:

$$\begin{bmatrix} \nabla^2 L & \nabla E^T & -I & I \\ \nabla E & 0 & 0 & 0 \\ Z_1 & 0 & Y & 0 \\ -Z_2 & 0 & 0 & (Y_{\max} - Y) \end{bmatrix}_{18n \times 18n} \begin{bmatrix} \Delta y \\ \Delta w \\ \Delta z_1 \\ \Delta z_2 \end{bmatrix} = - \begin{bmatrix} \nabla f + \nabla E^T W - z_1 + z_2 \\ E \\ Y Z_1 e - \mu e \\ (Y_{\max} - Y) Z_2 e - \mu e \end{bmatrix} \tag{3.15}$$

notice that the Jacobian matrix of System (3.15) is non-symmetric and highly indefinite.

The standard Newton's method assumptions for the convergence [26] of problem (3.11) are given by:

1. There exists $\nu^* = (y^*, w^*, z_1^*, z_2^*)$, solution to problem (3.11).

2. The Jacobian matrix $F'_\mu(\nu^*)$ is nonsingular.

3. The Jacobian operator F'_μ is locally Lipschitz continuous at ν^*.

In order to work with a smaller system, we derive a reduced system associated with (3.15). We write explicitly the equations of (3.15) as follows:

$$\nabla^2 L\Delta y + \nabla E^T \Delta w - \Delta z_1 + \Delta z_2 = -\left(\nabla f + \nabla E^T W - z_1 + z_2\right), \tag{3.16}$$

$$\nabla E \Delta y = -E, \tag{3.17}$$

$$Z_1 \Delta y + Y \Delta z_1 = -\left(Y Z_1 e - \mu e\right), \tag{3.18}$$

$$-Z_2 \Delta y + (Y_{\max} - Y)\Delta z_2 = -\left((Y_{\max} - Y) Z_2 e - \mu e\right). \tag{3.19}$$

Solving for Δz_1 in (3.18) and Δz_2 in (3.19), we get:

$$\begin{aligned} \Delta z_1 &= -z_1 + \mu Y^{-1} e - Y^{-1} Z_1 \Delta y, \\ \Delta z_2 &= -z_2 + \mu (Y_{\max} - Y)^{-1} e + (Y_{\max} - Y)^{-1} Z_2 \Delta y. \end{aligned} \tag{3.20}$$

By replacing (3.20) into (3.16), we get the reduced system:

$$\begin{bmatrix} \nabla^2 L + Y^{-1} Z_1 + \hat{Y} Z_2 & \nabla E^T \\ \nabla E & 0_{3n \times 3n} \end{bmatrix}_{8n \times 8n} \begin{bmatrix} \Delta y \\ \Delta w \end{bmatrix} = \begin{bmatrix} -\nabla f - \nabla E^T W - \mu \hat{Y} e \\ -E \end{bmatrix}, \tag{3.21}$$

where $\hat{Y} = (Y_{\max} - Y)^{-1}$. Therefore, the reduced system of equations (3.21) has some advantages over (3.15) including that the Jacobian is symmetric and likely to be positive definite as we add a positive definite matrix. Moreover, there is a considerable size reduction in the system being solved $(8n \times 8n)$ in comparison to $(18n \times 18n)$.

We use a *path-following* strategy [5, 6] to solve (3.21). For a $\mu > 0$ and working from the interior $(y_{\max} - y, z) > 0$, we apply a line-search Newton's method [45] to the perturbed KKT conditions (3.14). An optimal solution is reached when the perturbation parameter μ goes to zero.

Now we present the primal-dual interior-point algorithm for the nonlinear programming problem (3.11).

Algorithm 2 Primal-Dual Interior-Point Algorithm

1: Consider an initial interior point $v_0 = (y_0, w_0, z_{1_0}, z_{2_0})$, i.e., $(y_0, \hat{y}_0, z_{1_0}, z_{2_0}) > 0$, where $\hat{y} = y_{\max} - y$. Choose $\sigma \in (0, 1)$.

2: **for** $k = 0, 1, 2 \ldots$ until convergence **do**

3: Set the perturbed parameter $\mu_k = \min(\sigma \frac{y_k^T z_{1_k}}{5n}, \sigma \frac{\hat{y}_k^T z_{2_k}}{5n})$.

4: Solve the reduced system (3.21) for $\Delta\nu = (\Delta y, \Delta w)$, and solve (3.20) for Δz_1 and Δz_2.

5: Maintain $y, \hat{y}, z_1, z_2$, positive. Calculate $\tilde{\alpha_k}$ according to $\tilde{\alpha}_k = \min(\tilde{\alpha}_{1_k}, \tilde{\alpha}_{2_k})$, where

$$\begin{aligned} \tilde{\alpha}_{1_k} &= \min\left(\frac{-1}{\min(Z_1^{-1}\Delta z_1, -1)}, \frac{-1}{\min(Y^{-1}\Delta y, -1)}\right), \\ \tilde{\alpha}_{2_k} &= \min\left(\frac{-1}{\min(Z_2^{-1}\Delta z_2, -1)}, \frac{-1}{\min(-\hat{Y}^{-1}\Delta y, -1)}\right) \end{aligned}$$

6: Force a descent direction, For $i = 0, 1, 2, \ldots,$ set $\alpha_{k+1} = \left(\frac{1}{2}\right)^i \tilde{\alpha}_k$ until

$$M(v_k + \alpha_{k+1}\Delta v) < M(v_k) + 10^{-4}\alpha_{k+1}\nabla M^T \Delta v$$

where $M = ||F_\mu||^2$, for F_μ as in (3.14).

7: Update $v_{k+1} = v_k + \alpha_{k+1}\Delta v$.

8: **If** $||F_\mu|| \leq \epsilon$, break, **end**

9: **end for**

The numerical results of selected simulations generated by the implementation of both Pontryagin's maximum principle and primal-dual interior-point method are discussed in the next section.

3.3 Numerical Results

The results of selected simulations generated by the implementation of the strategies described in Chapter 2 using Forward-Backward (FB) and Primal-Dual Interior-Point Method (IPM) are presented in this section. We use a moderate value for the basic reproductive number $R_0 = 1.5$ and a final time of 220 days (number of days that the epidemic remains in

the population). We solve Problem (2.5),

$$\text{minimize } \frac{1}{2}\sum_{t=0}^{n-1}\left(B_1 I_t^2 + B_2 x_t^2 + B_3 \tau_t^2\right)$$

$$\text{subject to Model 3.6,}$$

$$0 \leq x_t \leq x_{\max},$$

$$0 \leq \tau_t \leq \tau_{\max},$$

using the strategies presented in Chapter 2: only social distancing, only treatment, and dual policies (social distancing and treatment). In Section 3.3.2 we present some numerical solutions using IPM for different scenarios. We study the impact of single and dual policies on the final epidemic size. The baseline parameter values are given in Table 3.1.

Table 3.1: Definition of parameters and baseline values.

Parameter	Value	Definition
σ_1	$\frac{1}{7}$	Recovering probability without treatment
σ_2	$\frac{1}{5}$	Recovering probability with treatment
ϵ	0.8	Transmissibility of the treated class
δ	0.001	Mortality rate
ρ	$0.19 - 0.41$	Susceptibility rate
n	220	Final time (days)

3.3.1 Comparison Between Forward-Backward and Primal-Dual Interior-Point Method

In this section, we show numerical simulations generated by solving problem (2.5) using the strategies presented in Chapter 2:

For Strategy 1 (social distancing): the antiviral treatment control $\tau_t = 0$,

For Strategy 2 (treatment): the social distancing control $x_t = 0$,

in the objective function F given in (3.4). The upper bounds for x_t and τ_t are $x_{\max} = 0.2$ and $\tau_{\max} = 0.2$ respectively; these values represent the maximum permitted value for each control policy daily; e.g. people can not reduce the number of contacts per day by more that 20% and the maximum number of infected individuals who get treatment is 20%. The weight constants B_1 to B_3, are a measure of the *relative* cost of interventions over $[0, n]$. In particular, B_2 and B_3, are the relative costs associated with the implementation of social distancing and antiviral treatment, respectively; we assume $B_2 > B_3$.

The weight constants are selected in part to facilitate computational issues. We carried out simulations under the assumption that the costs associated with social distancing (B_2) are higher than those associated with treatment (B_3). In this particular case we consider $B_1 = 20$, $B_2 = 0.2$, and $B_3 = 0.1$. In this experimentation, the basic reproductive number is $R_0 = 1.5$. The numerical results are presented in Table 3.2. For each strategy, we tabulate the number of iterations and the value of the functional at the optimal solution (F^*) by using FB and IPM algorithms. It should be noted that we do not compare CPU time since both algorithms ran within less than two seconds.

Table 3.2: Comparison between Forward-Backward and Primal-Dual Interior-Point Method.

	Algorithm1: FB		Algorithm2: IPM	
Strategy	# of iterations	F^*	# of iterations	F^*
1 - Social Distancing	52	0.67997	15	0.68001
2 - Treatment	54	0.33014	12	0.33016
3 - Dual Policies	87	0.30423	23	0.30092

In Table 3.2, we observe that for all strategies IPM requires fewer iterations to reach the solution with a competitive function value at the solution, when compared to FB.

Figures 3.2-3.4 show the level of intervention needed to control the epidemic and the final epidemic size with and without interventions for both methods for $R_0 = 1.5$.

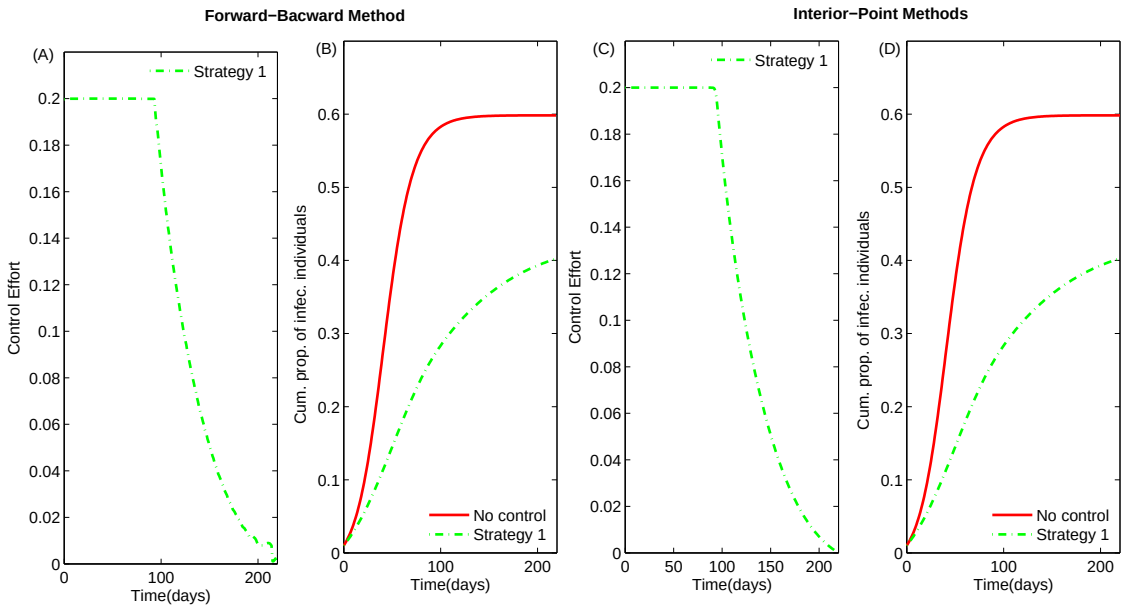

Figure 3.2: Strategy 1 (Social distancing): Figures A and B show the solution using FB and Figures C and D show the solution using IPM. Figures A and C are the optimal control solutions for each methodology, and Figures B and D illustrate the final epidemic size with and without control. The figures demonstrate the behavior is the same for both methods.

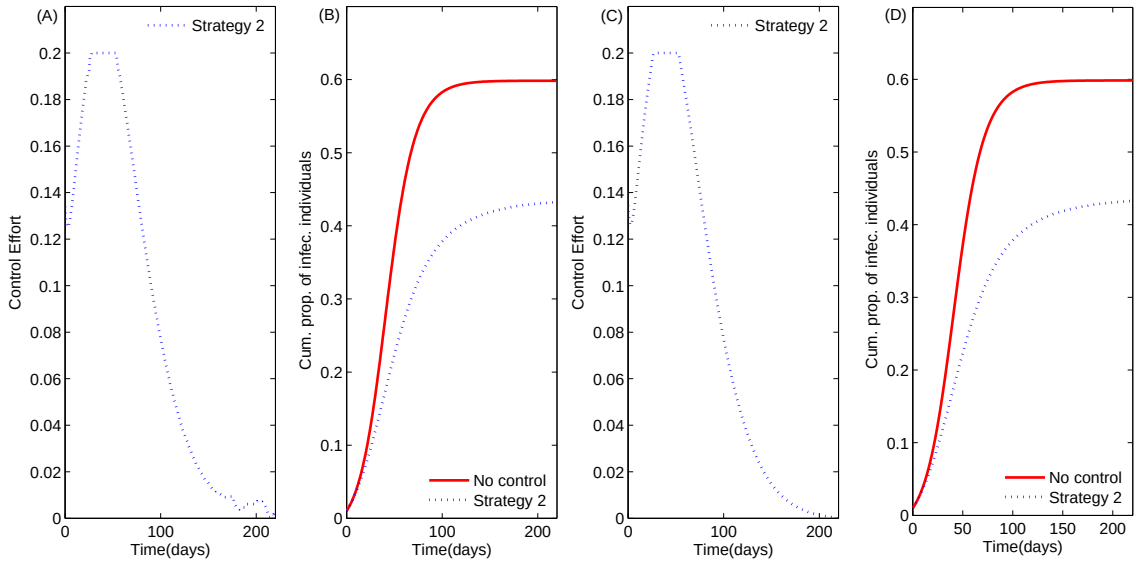

Figure 3.3: Strategy 2 (Treatment): the solutions using FB algorithm are presented in Figures A and B, and the solutions using IPM are shown in Figures C and D. The optimal control solutions are shown in plots A and C, while the final epidemic size with and without control are shown in Figures B and D. The figures show the same behavior for both methods.

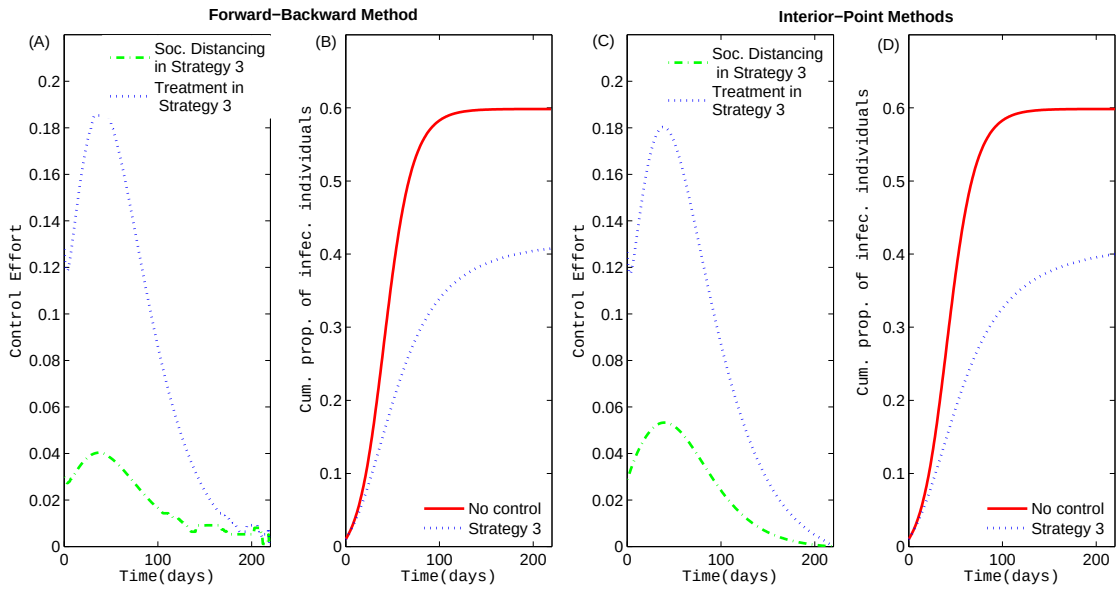

Figure 3.4: Strategy 3 (Social distancing and treatment): Figures A and B show the solutions using FB and Figures C and D illustrate the solution using IPM. Figures A and C show the optimal control solutions and Figures B and D show the final epidemic size with and without control.

3.3.2 Implication of Strategies

In this section, we present a comparison between strategies described in Chapter 2. The cumulative number of infected individuals for different values of R_0 in the absence of controls is compared against the presence of single or dual optimal controls. For single policies, a sensitivity analysis is carried out over the weight constants B_2 and B_3. In our simulations, we assume that the costs associated with social distancing are higher than those associated with treatment, i.e., $B_2 > B_3$. We compare the reduction in the final size as a result of the implementation of Strategies 1 through 3. In these simulations, the values for the weight constants are $B_2 = 0.2$ and $B_3 = 0.1$. Results for low to high values of R_0 are presented in Figure 3.5. Notice that the final epidemic size is reduced for all intervention strategies. The greatest reduction is obtain when Strategy 3, (social distancing and treatment) is implemented.

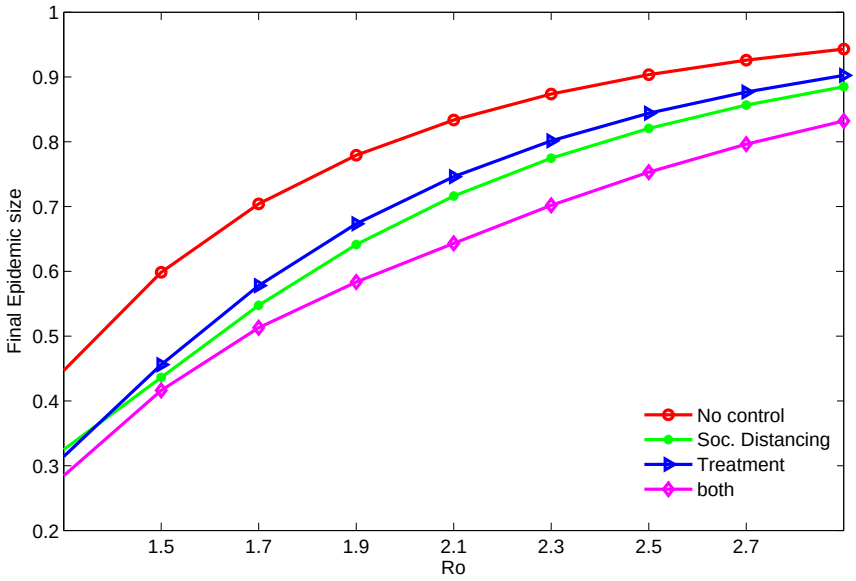

Figure 3.5: For different values of R_0, we show the final epidemic size under each strategy. We observe that dual policies (strategy 3) provides the greatest reduction in the final epidemic size. Notice that when $R_0 \geq 1.4$, social distancing give us a better reduction than treatment.

For single policies, Figure 3.5 shows that social distancing (Strategy 1) is better than

treatment (Strategy 2) for values of R_0 greater than 1.4. The results for $R_0 = 2.5$ are given in Figure 3.7. In this case, the optimal control solution for all strategies requires the maximum allowed value. The reduction in the final epidemic size for each strategy is summarized in Table 3.3.

Table 3.3: Comparison of strategies for low and moderate values of R_0 in reducing the final epidemic size.

Strategy	Reduction for $R_0 = 1.5$	Reduction for $R_0 = 2.5$
1	28%	12%
2	25%	7%
3	32%	18%

Finally, we explore the quantitative impact of the weight constants in terms of the reduction in the cumulative infected individuals and final epidemic size. We study the impact of three different values for B_2 and B_3 on Strategies 1 (social distancing) and 2 (antiviral treatment), respectively. We set $R_0 = 1.8$, $x_{\max} = 0.25$, and $\tau_{\max} = 0.25$.

Figures 3.8 and 3.9 show the optimal control solutions computed under strategies 1 and 2 as well as their impact on the cumulative proportion of infected individuals. Figure 3.8(A) shows that when the weight constant is small, $B_2 = 0.1$ (*relatively cheap*), the optimal control solution attains the maximum allowed value for social distancing within the first 110 days of the epidemic. This high value for the social distancing control, yields the highest reduction of 27% on the final epidemic size (Figure 3.8(C)). When the weight constant $B_2 = 0.2$ (*moderate cost*), the reduction on the final epidemic size is 24%. However, if the weight constant is increased to $B_2 = 1$ (*relatively expensive*), the reduction on the final epidemic size decreases by 13%. Figure 3.8(B) shows the reduction on the peak of the epidemic as the value of the weight constant B_2 decreases. When Strategy 2 is applied, similar results are obtained. As the weight constant B_3 increases, reductions on the final epidemic size are

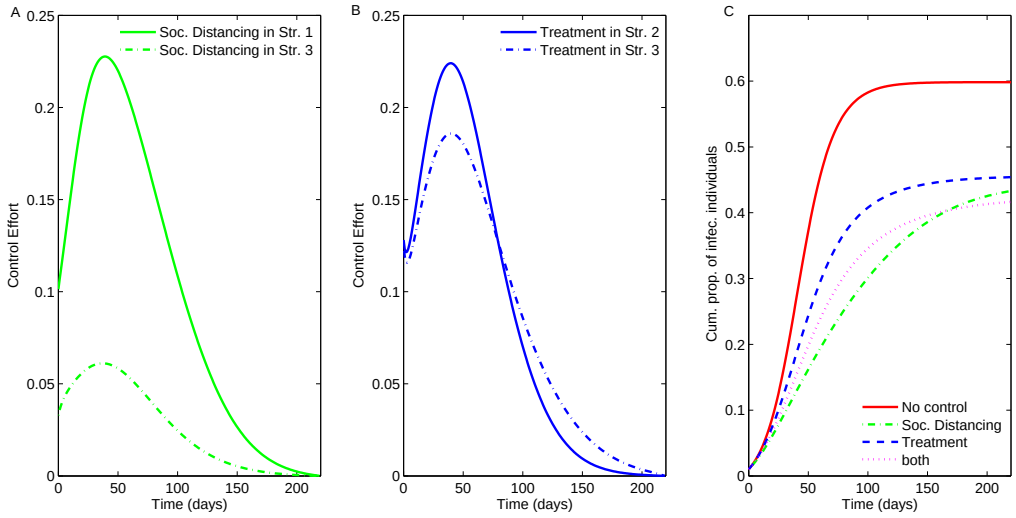

Figure 3.6: For $R_0 = 1.5$, the optimal control solution for each strategy is given in Figures A and B. The final epidemic size is reduced under the implementation of each strategy. For dual policies (treatment and social distancing), we get a reduction of 32%. The reduction for strategies 1 (social distancing) and 2 (treatment) are 28% and 25%, respectively.

observed. For example, when $B_3 = 0.01$, the reduction on the final epidemic size is 23% but when $B_3 = 1$ the reduction is only 10%. These results are summarized in Table 3.4.

Table 3.4: Different weight constants in Strategies 1 and 2

Strategy 1		Strategy 2	
B2	Final epidemic size reduction	B3	Final epidemic size reduction
0.1	27%	0.1	23%
0.2	24%	0.2	21%
1	13%	1	10%

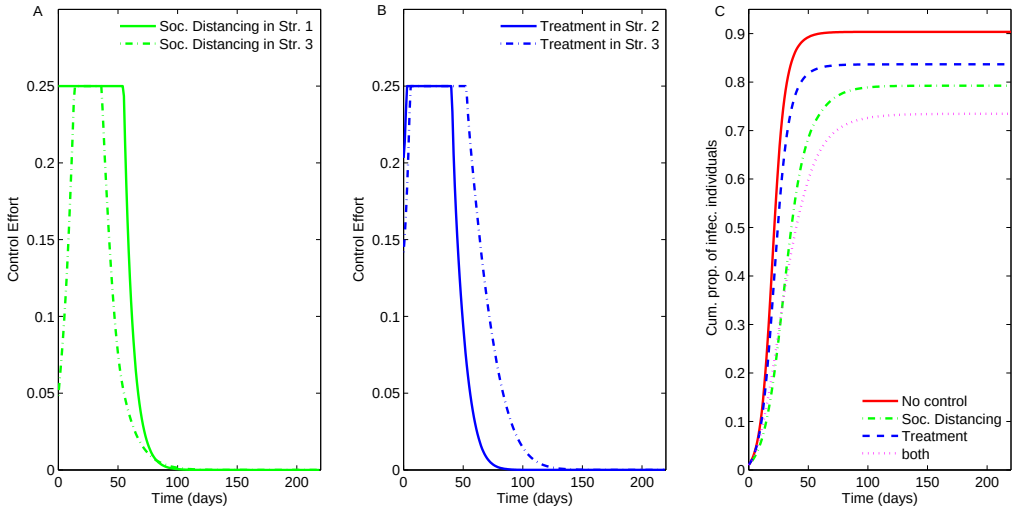

Figure 3.7: For $R_0 = 2.5$, the optimal control solution for each strategy requires the maximum permitted values. The final epidemic size is reduced by 18% in strategy 3 (treatment and social distancing). For strategies 1 (social distancing) and 2 (treatment), the reductions are 22% and 7%, respectively.

Summary of contribution: the contribution of this chapter is the formulation of an optimal control epidemiological model as a nonlinear programming problem. With this formulation, we were able to solve the problem by using primal-dual interior-point method for different strategies and considering different scenarios. We found that the use of single and dual strategies (social distancing and antiviral treatment) reduced the cumulative number of infected individuals. We have seen that dual strategies are more efficient at reducing the final epidemic size than single policies.

In the next chapter, we generalize our epidemiological model in order to formulate a group-structured model. The main idea is to consider some individuals' demographic characteristics and behavior. We introduce an optimal control problem associated with this group-structured model, and our goal is to determine how control policies should be applied in each group in order to reduce the number of infected individuals.

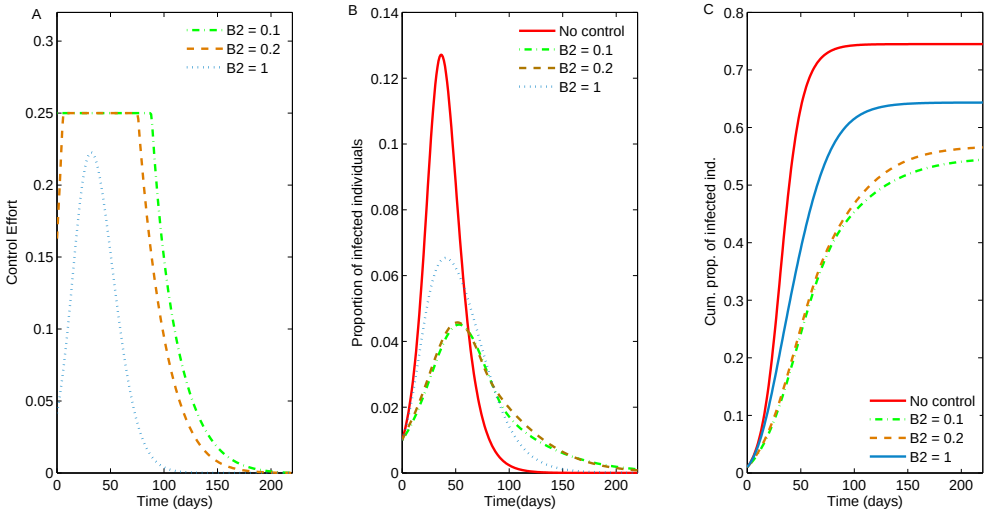

Figure 3.8: For different values of the weight constant B_2, Figures A and B show the optimal control solution when strategy 1 is applied. Figure C shows the corresponding final epidemic size. When $B_2 = 0.1$, we get a significant reduction of 28%.

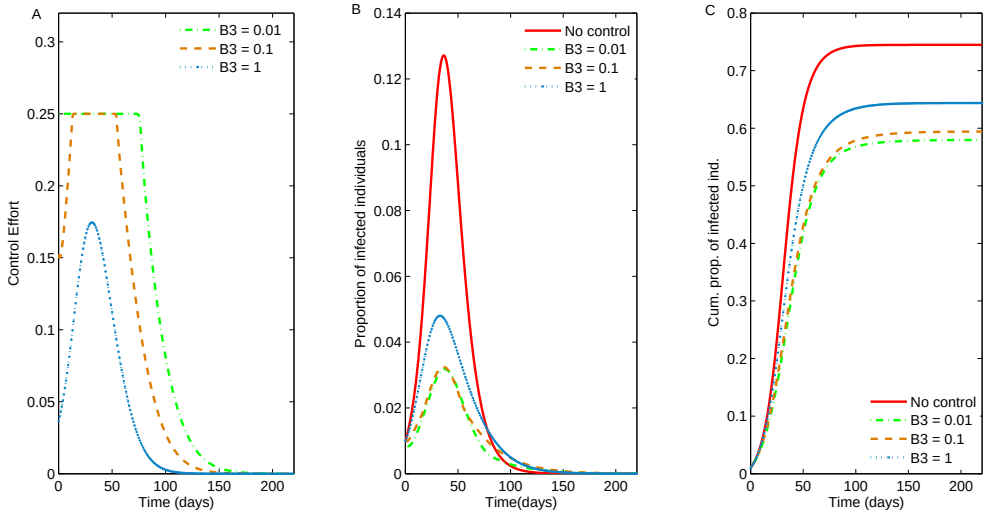

Figure 3.9: For strategy 2, Figure A shows the optimal control solution for different values of the weight constant B_3. Figure C shows the corresponding final epidemic size. When $B_3 = 0.01$, we get a reduction of 23%.

Chapter 4

Group-Structured Model

4.1 Formulation of the More General Problem

The dynamics of many diseases such as measles and influenza are strongly correlated with age [17], in this chapter we extend Model (2.1) by dividing the population into m age groups. Groups can be defined according to contact activity or susceptibility levels. We assume that people mix homogeneously within their group and proportionally between groups; this is known as proportionate mixing [12]. Epidemiological models with age structure have been considered for the continuous case in [17, 24, 30].

Let $N_i(t)$ be the number of individuals in group i at time t, $(i = 1, 2, \ldots, m)$ and q_{ij} be the probability that somebody from Group i has contact with somebody from group j. If we assume that both groups are connected $(q_{ij} > 0)$ and we consider proportionate mixing [17], we have

$$q_{ij} = q_j = \frac{C_j N_j}{\sum_{k=1}^{m} C_k N_k}, \tag{4.1}$$

where C_i is the average number of contacts per unit of time. Now we generalize the single population model SIR model (2.1) to a m-group model. Let $S_i(t)$, $I_i(t)$, and $R_i(t)$ denote the number of susceptible, infectious, and recovered individuals in the ith group, $i = 1, 2, \ldots, m$. We consider a single outbreak and people remain in the same group. We assume that infectious individuals from group i naturally recover with probability σ_i. The fraction of susceptible individuals on group i at time t that get infected at time $t + 1$ is modeled by the

function:

$$G_i(t) = \rho_i \sum_{j=1}^{m} \left(q_j \frac{I_j(t)}{N_j(t)} \right), \tag{4.2}$$

where ρ_i is the susceptibility rate for individuals in group i. The model is given by the system of difference equations:

$$\begin{aligned} S_i(t+1) &= S_i(t)(1 - G_i(t)) \\ I_i(t+1) &= S_i(t)G_i(t) + (1 - \sigma_i)\, I_i(t) \\ R_i(t+1) &= R_i(t) + \sigma_i I_i(t). \end{aligned} \tag{4.3}$$

Model (2.1) formulated in Chapter 2 is a particular case of Model (4.3) in the case of one group ($m = 1$). The basic reproductive number is calculated by using the next generation operator [2], it is given by

$$R_0 = \sum_{i=1}^{m} \frac{\rho_i q_i}{1 - (1 - \sigma_i)}.$$

Notice that there is a contribution from each group: it highlights that new infections can be generated from infected individuals on any group. There is a value of R_0 in each group which is calculated by using the expression given in (2.2), this values is different for each group since

The next step is to include treatment and social distancing as control policies in Model (4.3), in a similar way that we included them in the single group model (2.1) in Chapter 2.

We consider that the fraction of infected individuals in group i who get treatment each generation is modeled by $\tau_i(t)$. The *social distancing control* function, $x_i(t)$, models the reduction in the number of contacts per unit of time from individuals in group i. We assume that individuals (from any group) who get treatment recover with probability σ. Since treated individuals are still infectious, the function G_i, given in (4.2), is modified as

$$G_i = \rho_i \sum_{j=1}^{m} \left(q_j (1 - x_j(t)) \left(\frac{I_j(t) + \epsilon_j T_j(t)}{N_j} \right) \right), \tag{4.4}$$

where ϵ_j represents the effectiveness of treatment for individuals on group j, with $0 < \epsilon_j \leq 1$.

The model with control is given by the following system of difference equations:

$$\begin{aligned} S_i(t+1) &= S_i(t)(1-G_i(t)) \\ I_i(t+1) &= S_i(t)G_i(t) + (1-\tau_i(t))\,(1-\sigma_i)\,I_i(t) \\ T_i(t+1) &= (1-\sigma)\,T_i(t) + \tau_i(t)\,(1-\sigma_i)\,I_i(t) \\ R_i(t+1) &= R_i(t) + \sigma_i I_i(t) + \sigma T_i(t). \end{aligned} \tag{4.5}$$

Now we introduce the optimal control problem associated with the group-structured model (4.5). Our goal is to minimize the number of infected individuals in each group over a finite interval $[0, n]$, by using the least amount of treatment and social distancing. Following the ideas from Chapter 2, we generalize the problem given in (2.5); therefore, the optimal control problem associated with the age-structured model can be written as:

$$\begin{aligned} &\text{minimize } \frac{1}{2}\sum_{i=1}^{m}\left(\sum_{t=0}^{n-1}\left(B_{I_i}I_i(t)^2 + B_{x_i}x_i(t)^2 + B_{\tau_i}\tau_i(t)^2\right)\right) \\ &\text{subject to Model (4.5),} \end{aligned} \tag{4.6}$$

where n and m denote the final time and the number of groups, respectively. The weight constants B_j, $(j = I_i, \tau_i, x_i)$ are a measure of the *relative* cost of interventions over $[0, n]$. In particular, B_{x_i} and B_{τ_i} denote the relative costs associated with the implementation of social distancing and antiviral treatment in group i, respectively.

The problem is solved by using the primal-dual interior-point method. In a similar way that we solved problem (2.5) in Chapter 3, we rewrite Problem (4.6) as a nonlinear programming problem:

$$\begin{aligned} \min \quad & f(y) \\ \text{s.t.} \quad & E(y) = 0, \\ & 0 \le y \le y_{\max}, \end{aligned} \tag{4.7}$$

where

$$\begin{aligned} \mathbf{y} = {} & (S_1(1), I_1(1), T_1(1), \tau_1(0), x_1(0), \ldots, S_1(n), I_1(n), T_1(n), \tau_1(n-1), x_1(n-1), \ldots \\ & S_m(1), I_m(1), T_m(1), \tau_m(0), x_m(0), \ldots, S_m(n), I_m(n), T_m(n), \tau_m(n-1), x_m(n-1))^T, \end{aligned} \tag{4.8}$$

m is the number of groups and n is the final time. The objective functional is given by:

$$f(y) = \frac{1}{2}\sum_{i=1}^{m}\left(B_{I_i}\|\tilde{I}_i\|^2 + B_{\tau_i}\|\tau_i\|^2 + B_{x_i}\|x_i\|^2\right),$$

$f : \mathbb{R}^{5\cdot n\cdot m} \to \mathbb{R}$, with $\tilde{I}_i = (I_i(0), I_i(1), \ldots, I_i(n-1))^T$, $\tau_i = (\tau_i(0), \tau_i(1), \ldots, \tau_i(n-1))^T$, and $x_i = (x_i(0), x_i(1), \ldots, x_i(n-1))^T$ for $i = 1, 2, \ldots, m$. From Model (4.5), we get the equality constraint $E : \mathbb{R}^{5\cdot n\cdot m} \to \mathbb{R}^{3\cdot n\cdot m}$,

$$E(y) = \begin{pmatrix} E_1(y) \\ E_2(y) \\ \vdots \\ E_m(y) \end{pmatrix}, \tag{4.9}$$

where

$$E_i(y) = \begin{pmatrix} S_i(1) - S_i(0)(1 - G_i(0)) \\ I_i(1) - S_i(0)G_i(0) - (1 - \tau_i(0))\,(1 - \sigma_i)\,I_i(0) \\ T_i(1) - (1 - \sigma)\,T_i(0) - \tau_i(0)\,(1 - \sigma_i)\,I_i(0) \\ \vdots \\ S_i(n) - S_i(n-1)(1 - G_i(n-1)) \\ I_i(n) - S_i(n-1)G_i(n-1) - (1 - \tau_i(n-1))\,(1 - \sigma_i)\,I_i(n-1) \\ T_i(n) - (1 - \sigma)\,T_i(n-1) - \tau_i(n-1)\,(1 - \sigma_i)\,I_i(n-1) \end{pmatrix}, \tag{4.10}$$

and G_i is given in (4.4). We solve problem (4.7) by using the primal-dual interior-point method presented in Chapter 3.

In the next section, we present the results of some numerical simulations in which we assume that the total population is divided into two groups. For this particular case, we consider only treatment as a control policy, under the assumption of unlimited supplies. In the next chapter, we study the case of limited resources by introducing an isoperimetric constraint [40, 42]. Finally, we analyze the case when the total population is divided into three groups; for this case social distancing and treatment are implemented simultaneously.

For each case, we consider that individuals remain in the same group, i.e. they do not change age.

4.2 Numerical Results: Two-Groups Model

In this section, we present some results of selected simulations under various scenarios. First, we consider both groups with the same population size. Then, we present a more realistic scenario with different population sizes in the case of seasonal influenza. For all simulations, we solve an optimal control problem by using the primal-dual interior-point method described by Algorithm 2. For each case, we compare the proportion of infected individuals generated in the absence or in the presence of control. In these simulations, the weight constants are selected, in part, to facilitate computational issues: interior-point methods are sensitive to these values. We assume a moderate value of R_0 $(1.5 - 1.7)$. The final time of 180 days is chosen for all simulations. The baseline parameter values are given in Table 4.1.

Table 4.1: Definition of parameters and baseline values.

Parameter	Value	Definition
σ_i	$\frac{1}{7}$	Recovering probability without treatment in Group $i = 1, 2$
σ	$\frac{1}{5}$	Recovering probability with treatment in all groups
ϵ	0.7	Transmissibility of the treated class
δ	0.001	Mortality rate due to the disease
ρ_i	$0.135 - 1.9$	Susceptibility rate for individuals in Group $i = 1, 2$
C_i	$0.003 - 0.01$	Average contact rate of individuals in Group $i = 1, 2$
B_j	$0.3 - 1$	Weight constants in the objective function, $j = \{I_i, \tau_i\}$ and $i = 1, 2$

By considering the case of unlimited doses of treatment, we divide the total population into two groups with same population size, and we consider three different scenarios. In the first scenario, both groups have the same activity and susceptibility levels; basically, we want to validate our IPM algorithm. As we described in the previous section, C_i and ρ_i are the

average contact and the susceptibility levels for individuals in group $i = 1, 2$, respectively. For the second scenario, we assume that Group 1 is more active than Group 2, hence the average contact number is higher in Group 1 than Group 2 ($C_1 > C_2$), and both groups have the same susceptibility level ($\rho_1 = \rho_2$). For both scenarios, Figures 4.1 - 4.4 show the control effort, the proportion of infected individuals, and the final epidemic size for Groups 1 and 2, respectively.

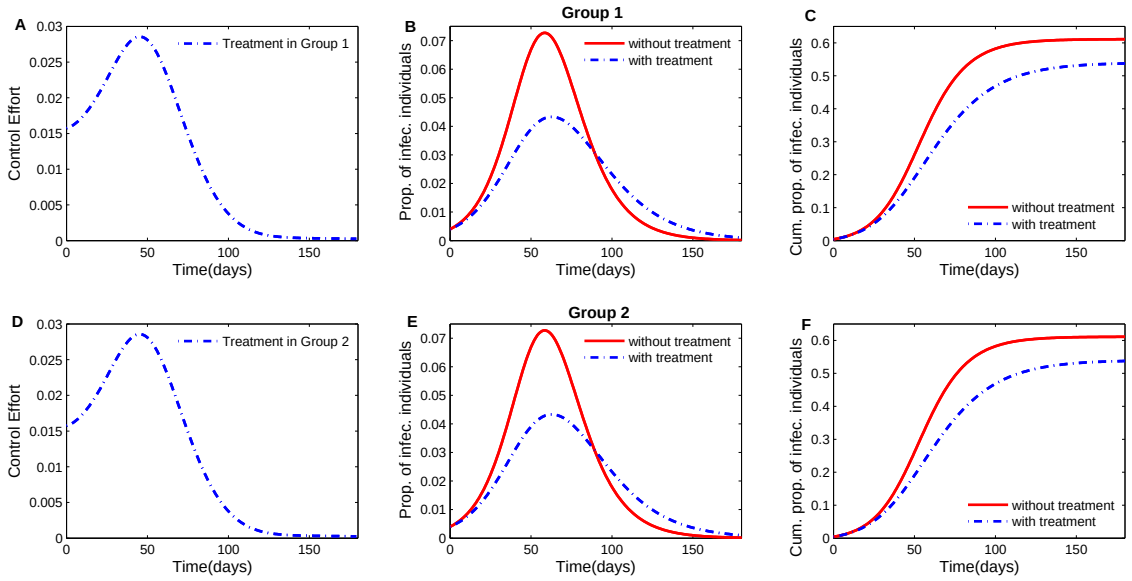

Figure 4.1: In the case of same population size in Groups 1 and 2, the first scenario considers both groups with the same susceptibility and same activity level. Since both groups have similar behavior, the optimal control strategy requires the implementation of the same amount of treatment in both groups. The final epidemic size is reduced by 14% in each group.

Scenario 1: Same Activity and Susceptibility Levels

Since both groups have the same population size and similar behavior, the optimal control solution requires the implementation of the same amount of treatment for both groups (Figures 4.1A and 4.1D), therefore we get the same reductions on the final epidemic size (14%) in each group, as shown in Figures 4.1C and 4.1F. The implementation of treatment shifts the

peak; without treatment, the epidemic peaks on day 50, while in the presence of treatment, it peaks on day 60 (Figures 4.1B and 4.1E).

Scenario 2: Same Activity Level, Higher Susceptibility in Group 1

Figures 4.2A and 4.2D show the optimal control solution when both groups have the same population size and activity levels, but Group 1 is more susceptible than Group 2. Since Group 1 has higher susceptibility; the optimal control solution requires the application of higher values of treatment in this group. The reduction in the final epidemic size is given by 11% and 13% in Groups 1 and 2, respectively (Figures 4.2C and 4.2F). This reduction is smaller in Group 1 because the number of infected individuals is higher in this group.

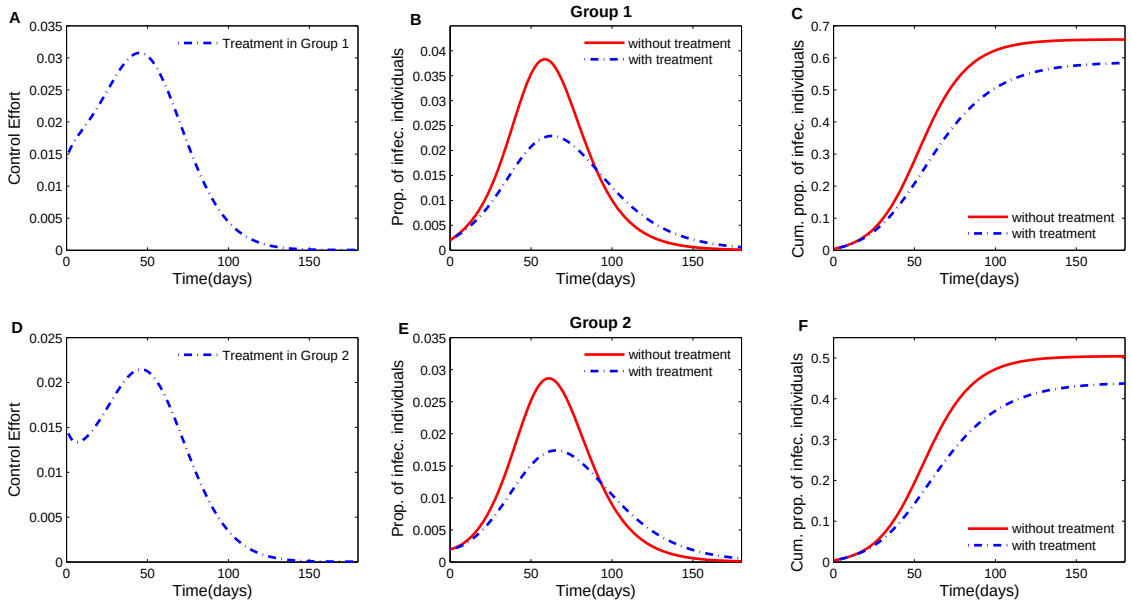

Figure 4.2: For Scenario 2, Group 1 is more susceptible than Group 2 but they have the same activity level. Since Group 1 is the high risk group, the optimal control strategy requires more resources for this group; however, the number of infected individuals is higher in Group 1 and the reduction on the final epidemic size will be larger in Group 2.

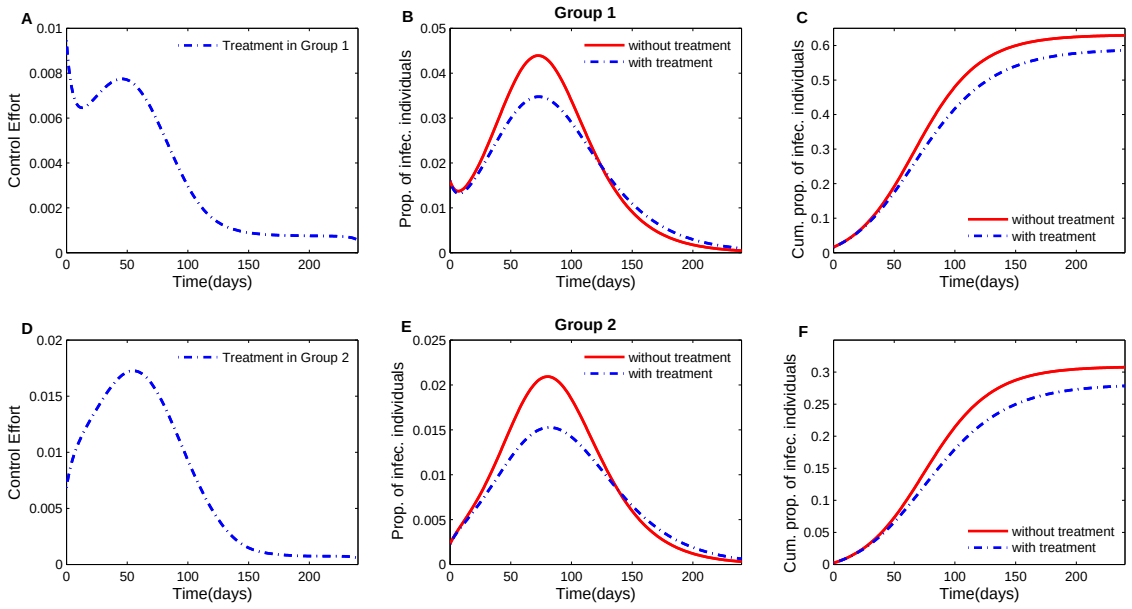

Figure 4.3: In the case of seasonal influenza, for Scenario 1, Group 1 (12.5 % of the total population) is the high risk population and both groups have the same activity level. Because of the population size, the amount of effort needed to control the epidemic is higher in Group 2 and therefore, the reduction on the final epidemic size is higher in Group 2 (25%) than Group 1 (10.7%).

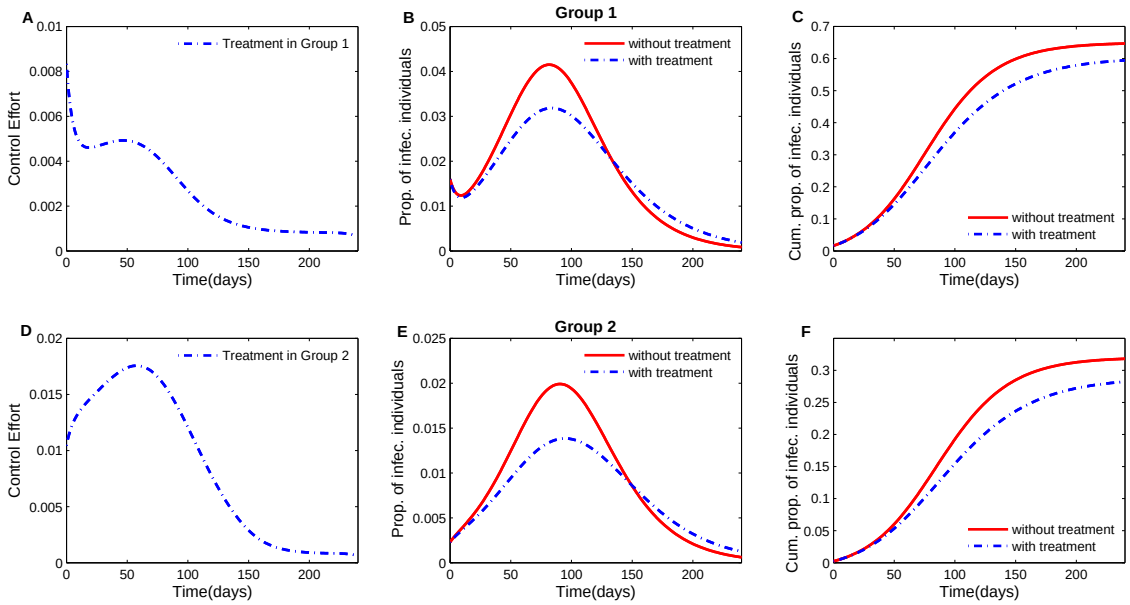

Figure 4.4: For seasonal influenza, in scenario 2, Group 1 (12.5 % of the population) is more susceptible but less active than Group 1. Since Group 2 is more active, more effort has to be applied in this group. Figure D shows that we need to apply twice the treatment for Group 2 than for Group 1 (Figure A).

4.2.1 Seasonal Influenza

In this section, we consider the case of seasonal influenza. We divide the total population into two groups with different population sizes. Group 1 is given by 12.5% of the population aged 65 or more, and Group 2 is 87.5% of the population aged less than 65 [12]. For these simulations we assume that $R_0 = 1.27$ and that Group 1 is the high risk population ($\rho_1 > \rho_2$). The final time (day when there were no more infected individuals) is 240 days. For Scenario 1, we assume same activity level ($C_1 = C_2$); for Scenario 2, we assume that Group 2 is more active than Group 1 ($C_2 > C_1$).

Scenario 1: High Susceptibility in Group 1 and Same Activity in Both Groups Figure 4.3 shows the results for Scenario 1. The optimal control solution shows that the amount of treatment that should be applied is higher in Group 2, because this group has a larger population size (Figures 4.3A and 4.3D). With the implementation of the optimal control treatment, the final epidemic size is reduced by 7% and 10% in Groups 1 and 2, respectively (Figures 4.3C and 4.3F).

Scenario 2: High Susceptibility and Low Activity Level in Group 1 The results for Scenario 2 are shown in Figure 4.4. Since we have Group 2 as the more active one, the optimal control requires more resources for this group than for Group 1; Figure 4.4D shows that we need to apply twice the treatment for Group 2 than for Group 1 (Figure 4.4A). The reduction on the final epidemic size is given by 8% and 12% in Groups 1 and 2, respectively.

4.3 Numerical Results: Three-Groups Model

In this section, we divided the population into three age groups. Group 1 is given by people between 0 and 19 years of age (27%), Group 2 is individuals between 20 and 64 (60%), and Group 3 is people aged 65 or more (13%). Figure 4.5 shows the number of individuals in each age group according to the 2010 US Census [19].

Since children and teenagers are in Group 1, we assume that this group has the highest

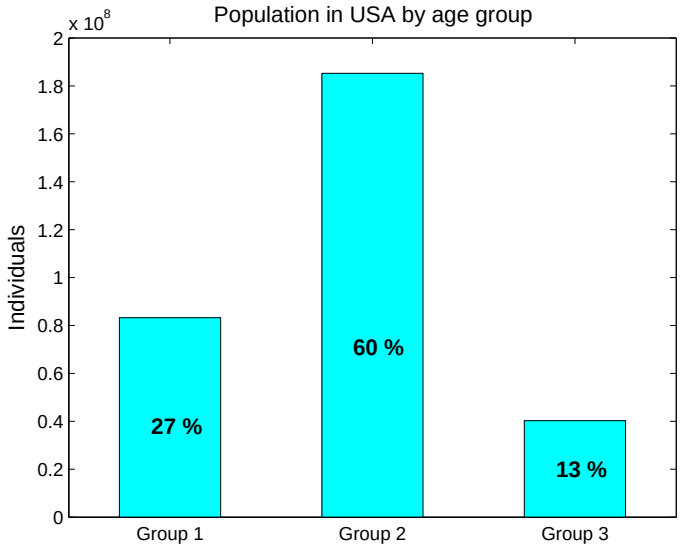

Figure 4.5: According to the 2010 US Census (27%) of the population is in Group 1, (60%) in Group 2, and (13%) in Group 3.

level of activity, while seniors (Group 3) is assumed to be the least active group [41, 53].

In these numerical simulations, the weight constants are selected, in part, to facilitate computational issues since interior-point methods are sensitive to these values. We consider a small $(1.2-1.35)$ and a moderate $(1.6-1.8)$ value for R_0 under both seasonal and pandemic H1N1 influenza. For all simulations, we solve an optimal control problem using the primal-dual interior-point method given in Algorithm 2. The final time is given by $n = 250$ in the case of small R_0 and $n = 180$ for a moderate value of R_0. The baseline parameter values are given in Table 4.4.

4.3.1 Seasonal Influenza

In the case of seasonal influenza, the high risk population is typically considered to be people over 65 (Group 3), followed by school-aged children (Group 1) ($\rho_3 > \rho_1 > \rho_2$). The size and behavior of each group is given in Table 4.2. We consider two scenarios: in the first one $R_0 = 1.22$, and in the second one $R_0 = 1.62$. Figures 4.6 and 4.7 show the results for both

scenarios. The top, middle, and bottom figures show the results for Groups 1-3 respectively.

Table 4.2: Characteristics of each group in the case of seasonal influenza.

Group	Age	Population Size	Susceptibility	Activity Level
1	$0-19$	27%	medium	high
2	$20-64$	60%	low	medium
3	65 and more	13%	high	low

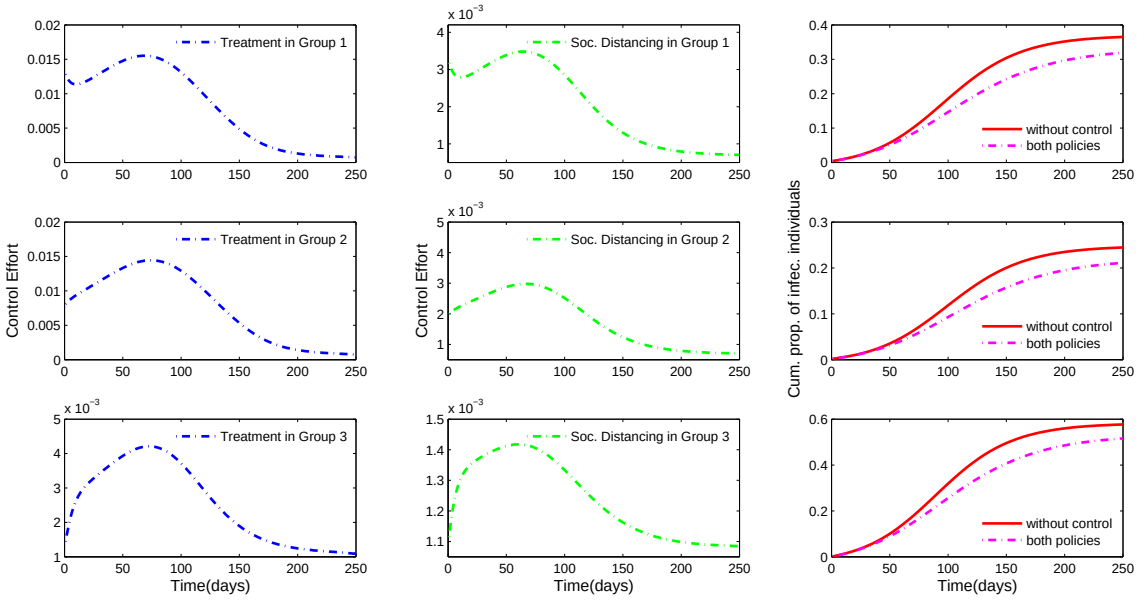

Figure 4.6: The largest amount of resources need to be channeled towards the highest risk population (Group 1) and the group with the largest population size (Group 2). The implementation of mitigation strategies reduce the final epidemic size by 13%, 14%, and 11% in Groups 1, 2 and 3, respectively.

For each group, we found the optimal control solution for treatment and social distancing, respectively and the proportion of infected individuals in each group. The optimal control solution shows that the largest amount of resources need to be used towards the high activity

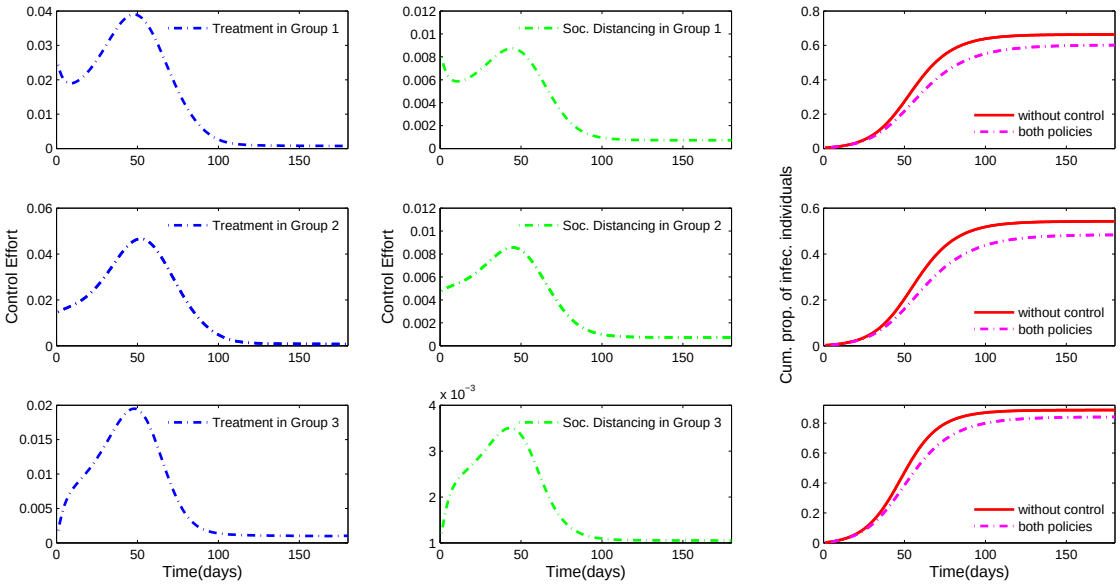

Figure 4.7: For a moderate value of R_0, the values of treatment and social distancing applied to each group are higher than the ones for the case of small R_0. The reduction on the final epidemic size is given by 9%, 11%, and 5% for each group.

level, i.e., to Group 1, followed by the group with the largest population, Group 2; however, the values of treatment and social distancing are close between Group 1 and 2. Although Group 3 has higher susceptibility, the treatment and social distancing values are smaller for this group. The fraction of individuals that get infected is larger for Group 3 since it has the highest susceptibility. The implementation of policies reduces the final epidemic size by 13%, 14%, and 11% in Groups 1, 2, and 3, respectively for the case of small R_0. In the case of a moderate value of R_0, the reduction is given by 9%, 11%, and 5% in each group respectively. For a moderate value of R_0, the optimal control solution requieres the implementation of higher values of treatment and social distancing in each group (Figure 4.7); however, the reduction on the final epidemic size is smaller than in the case of small R_0.

4.3.2 Influenza H1N1

In contrast with seasonal influenza, the estimated number of 2009 H1N1 cases is higher in Group 2, while lower in Group 3 [18]. Therefore, in these simulations we consider Group 2 as the highest risk group while Group 3 is the lowest risk, in addition, the mortality due to the disease is also higher in Group 2 [18]. Figures 4.8 and 4.9 show the results for two scenarios: $R_0 = 1.32$ and $R_0 = 1.66$. The top, middle, and bottom sets of figures show the results in Groups 1-3. For each group, the figures show the optimal control solution for treatment and social distancing, respectively and the proportion of infected individuals in each group. The size and behavior of each group is given in Table 4.3.

Table 4.3: Characteristics of each group in the case of H1N1 influenza.

Group	Age	Population Size	Susceptibility	Activity Level
1	$0-19$	27%	medium	high
2	$20-64$	60%	high	medium
3	65 and more	13%	low	low

In the case of small R_0, Figure 4.8 shows that the optimal control solution requires

the maximum amount of treatment and social distancing applied towards the high risk population, Group 2, followed by Group 1. Since Group 2 is both the highest risk and has the largest population size, the values of social distancing and treatment are much greater that the ones for Group 1. Since Group 3 is the group with the lowest risk and has the smallest population size, the optimal control solution requires the implementation of the lower values of treatment and social distancing. The implementation of control policies reduces the final epidemic size by 7%, 6%, and 8%. Notice that since Group 3 has the smallest population and is the lowest risk group, the reduction on the final epidemic size is higher in this group, even though the values of treatment and social distancing are lower for this group.

In the case of moderate value of R_0, Figure 4.9 shows results which are similar to the results corresponding to small R_0. The largest amount of resources for both social distancing and treatment have to be channeled towards the high susceptibility Group 2, followed by Groups 1 and 3, respectively. The optimal control solution for treatment has similar values for Groups 1 and 3; however, since Group 1 has the highest activity level, the social distancing in Group 1 is 10 times the one in Group 3. The final epidemic size is reduced by 11%, 8%, and 13% in Groups 1, 2, and 3, respectively.

Finally, we compare strategies implemented during seasonal and pandemic influenza. Figure 4.10 shows how control policies should be implemented in each group both in the case of seasonal and pandemic influenza; in particular, it shows how treatment doses should be distributed in the case of small and moderate values of R_0. Since Group 2 has the largest population size, more treatment doses have to be used in this group. In the case of H1N1, the number of doses needed for Group 2 is higher than in the case of seasonal influenza, because this group is the highest risk group for H1N1. In contrast, the number of doses in Groups 1 and 3 are higher in the case of seasonal influenza than in the case of H1N1. Therefore, in the presence of a new pandemic, the implementation of policies should be analyzed for that particular case and the new polices are not necessarily the same as in the case of seasonal influenza.

Summary of contribution: the formulation of a discrete group-structured influenza model is the main contribution of this chapter. Previous research of age-structured influenza models have been used for the continuous case. We formulated an age-structured optimal control model and solved it using interior-point methods. In particular, we considered two and three groups for both seasonal and pandemic influenza.

In all of the previous simulations, we assumed the ideal case of unlimited resources. In the next chapter, we study the case of limited resources, which is a more realistic scenario. Therefore, we will modify our optimal control problem by including an isoperimetric constraint which represent the available doses of treatment. The new problem will be solved by using interior-point methods.

Table 4.4: Definition of parameters and baseline values in the case of three groups.

Parameter	Value	Definition
σ_i	$\frac{1}{7}$	Recovering probability without treatment in Group $i = 1, 2, 3$
σ	$\frac{1}{5}$	Recovering probability with treatment in each group
ϵ	0.7	Transmissibility of the treated class
δ_1	6.4×10^{-5}	Mortality rate due to the disease in Group 1
δ_2	2.8×10^{-4}	Mortality rate due to the disease in Group 2
δ_3	2.7×10^{-4}	Mortality rate due to the disease in Group 3
ρ_1	$0.12 - 0.25$	Susceptibility rate for individuals in Group 1
ρ_2	$0.13 - 0.32$	Susceptibility rate for individuals in Group 2
ρ_3	$0.06 - 0.5$	Susceptibility rate for individuals in Group 3
C_i	$0.003 - 0.01$	Average contact rate of individuals in Group $i = 1, 2, 3$
B_{I_j}	1	Weigh constants in the objective function, $i = 1, 2, 3$
B_j	$0.07 - 0.4$	Weigh constants in the objective function, $j = x_i, \tau_i$, $i = 1, 2, 3$

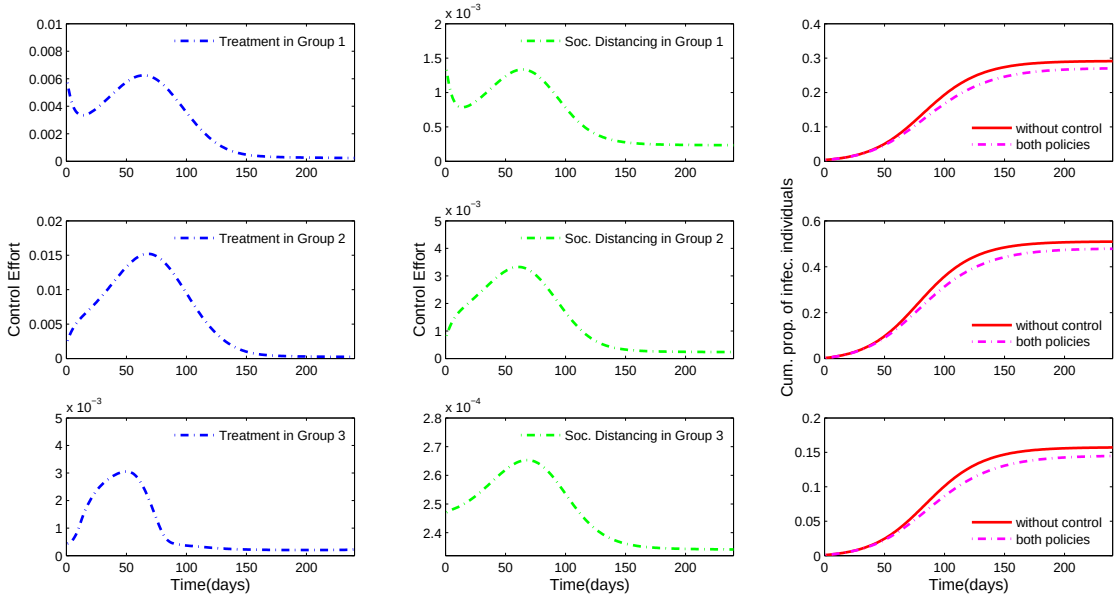

Figure 4.8: In the case of influenza H1N1 and $R_0 = 1.32$, the optimal control solution shows that the largest amount of resources for treatment and social distancing has to be channeled towards the highest risk Group 2. The final epidemic size is reduced by 7%, 6%, and 8% in Groups 1, 2 and 3, respectively.

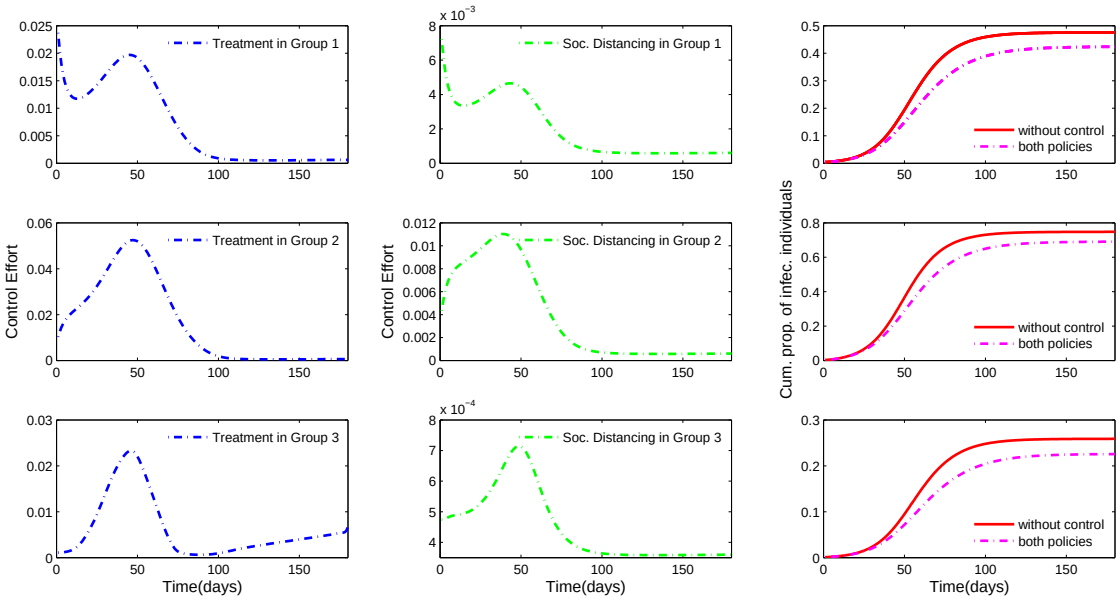

Figure 4.9: For Influenza H1N1 and a moderate value of $R_0 = 1.66$, the values of treatment and social distancing used for each group are higher than the ones in the case of small R_0. The largest amount of resources had to be channeled towards the high risk Group 2. The reduction on the final epidemic size is given by 11%, 8%, and 13% in each group.

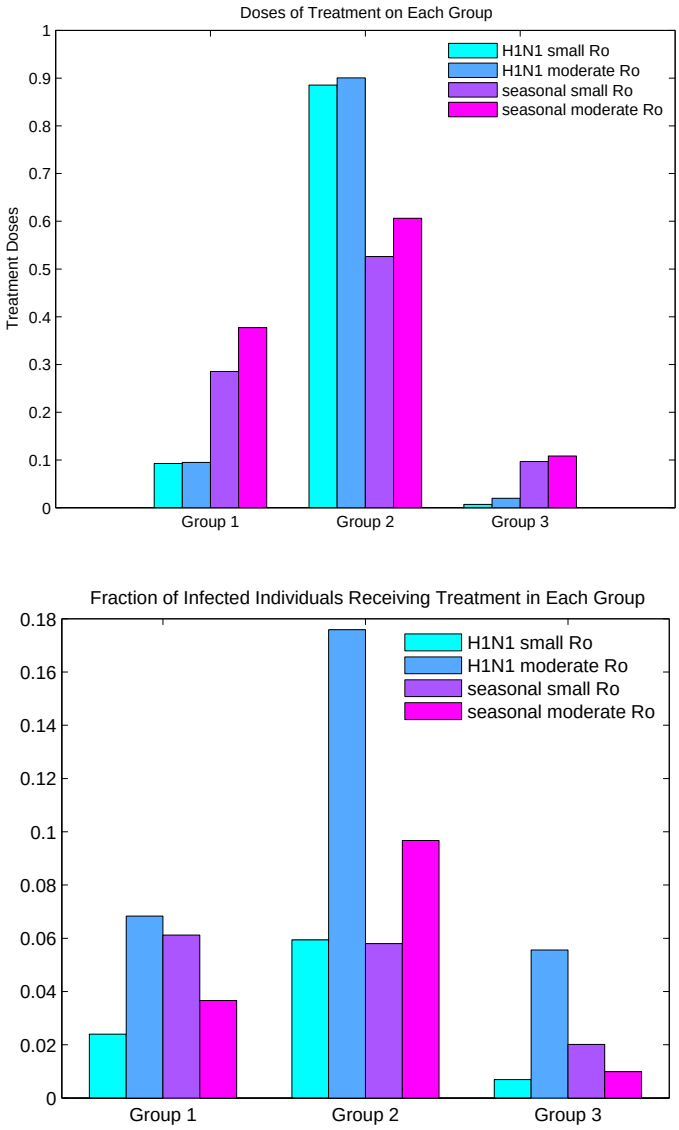

Figure 4.10: Top figure shows that since 60% of the population is in Group 2, a high number of doses has to be used for this group. This number is higher in the case of influenza H1N1 than in the case of seasonal influenza because Group 2 is the high risk population for H1N1. For Groups 1 and 3 (27% and 13% of the population respectively) the number of doses is higher for seasonal influenza than for H1N1. The bottom figure contrasts the results we reported in the top figure but showing the fraction of treatment doses per infected individual per group.

Chapter 5

When Resources are Limited

5.1 Problem Formulation

In the previous chapter we considered the ideal case of unlimited doses of treatment and solved problem (4.7) when the total population is divided into two or three groups. In this chapter, we consider a more realistic scenario when treatment supplies are limited. We modify Problem (4.7) by including the "isoperimetric" constraint [40, 42]

$$\sum_{i=1}^{m}\left(\sum_{t=0}^{n-1}(\tau_i(t)I_i(t))\right)=k, \tag{5.1}$$

where k represents the available number of treatment doses, n the final time, and m the number of groups. Notice that (5.1) can be written as the inner product of $\boldsymbol{\tau}_i$ and $\tilde{\mathbf{I}}_i$, $(i=1,2,\ldots,m)$

$$\sum_{i=1}^{m}\boldsymbol{\tau}_i^T\tilde{\mathbf{I}}_i-k=0, \tag{5.2}$$

where $\boldsymbol{\tau}_i=(\tau_i(0),\tau_i(1),\ldots,\tau_i(n-1))$ and $\tilde{\mathbf{I}}_i=(I_i(0),I_i(1),\ldots,I_i(n-1))$.

A similar problem has been solved in [40] by considering limited vaccine in a continuous time influenza model. The problem was solved by including a new state variable related to the isoperimetric constaint, which requires boundary conditions at $t=0$ and $t=n$; In this case, Pontryagin's maximum principle cannot be used directly, as shown in Section 3. The authors of [40] remark that since we include the isoperimetric constraint, convergence issues have to be addressed. We will solve the new problem by using the primal-dual interior-point method, which allows the inclusion of the new constraint more efficiently.

The optimal control problem can be written as:

$$\begin{aligned} \min \quad & f(y) \\ \text{s.t.} \quad & E(y) = 0, \\ & 0 \leq y \leq y_{\max}, \end{aligned} \tag{5.3}$$

where

$$\begin{aligned} \mathbf{y} \;=\; & (S_1(1), I_1(1), T_1(1), \tau_1(0), \ldots, S_1(n), I_1(n), T_1(n), \tau_1(n-1), \ldots \\ & S_m(1), I_m(1), T_m(1), \tau_m(0), \ldots, S_m(n), I_m(n), T_m(n), \tau_m(n-1))^T, \end{aligned} \tag{5.4}$$

m is the number of groups and n is the final time. The objective functional is given by:

$$f(y) = \frac{1}{2} \sum_{i=1}^{m} \left(B_{I_i} \|\tilde{I}_i\|^2 + B_{\tau_i} \|\tau_i\|^2 \right),$$

$f : \mathbb{R}^{4 \cdot n \cdot m} \to \mathbb{R}$, with $\tilde{I}_i = (I_i(0), I_i(1), \ldots, I_i(n-1))^T$, $\tau_i = (\tau_i(0), \tau_i(1), \ldots, \tau_i(n-1))^T$, and $x_i = (x_i(0), x_i(1), \ldots, x_i(n-1))^T$ for $i = 1, 2, \ldots, m$.

We obtain the equality constraint $E : \mathbb{R}^{4 \cdot n \cdot m} \to \mathbb{R}^{3 \cdot n \cdot m + 1}$ by including the isoperimetric constraint (5.2) into the equality constraint given in (4.9), therefore E is given by:

$$E(y) = \begin{pmatrix} E_1(y) \\ E_2(y) \\ \vdots \\ E_m(y) \\ \boldsymbol{\tau}_1^T \tilde{\mathbf{I}}_1 + \cdots + \boldsymbol{\tau}_m^T \tilde{\mathbf{I}}_m - k \end{pmatrix}, \tag{5.5}$$

where E_i is given by (4.10).

By using the primal-dual interior-point method, given in Algorithm 2 we solve Problem (5.3) for two particular cases. In the first case, we consider just one group ($m = 1$); in the second case, the total population is divided into two subgroups ($m = 2$). In the next section, we present the results of selected numerical simulations.

5.2 Numerical Simulations: One-Group Model

In the case of one-group model, we solve the problem by considering two different values of R_0. In the first scenario $R_0 = 1.5$, the final time is $n = 200$; in the second scenario $R_0 = 2.6$ and $n = 120$. Since we are considering a single epidemic outbreak when R_0 increases, the final time reduces because the epidemic ends sooner. The baseline parameter values are given in Table 3.1. The values of weight constants are $B_I = 10$ and $B_\tau = 0.1$. The isoperimetric constraint k represents the doses availability. In our simulations, k is a value between 10% and 80%, which represents the percentage of infected individuals that get treatment during the full epidemic period. For each scenario we solve the problem for four different values of k. The primal-dual interior-point method allows convergence for smaller values of k than the ones used in [40].

For both scenarios, Figures 5.1 and 5.2 show the optimal control solution on the left and the cumulative number of infected individuals on the right, for different values of k. For small values of k, the optimal control solution requires the largest amount of resources at the beginning of the epidemic until the resources are exhausted.

For $R_0 = 1.5$, we consider cases when treatment doses are availables for $53\%, 37\%, 25\%$, and 10% of the infected individuals, Figure 5.1 (right) shows that the implementation of optimal control strategies reduce the final epidemic size by $28\%, 18\%, 12\%$, and 5%, respectively.

Figure 5.2 presents the results for $R_0 = 2.6$. In this case, the optimal control solution requires the largest values of treatment, and the reduction on the final epidemic size is smaller than the case of $R_0 = 1.5$. The reduction on the final epidemic size is $11\%, 7\%, 5\%$, and 1% with treatment doses available for $80\%, 60\%, 46\%$, and 11%, respectively.

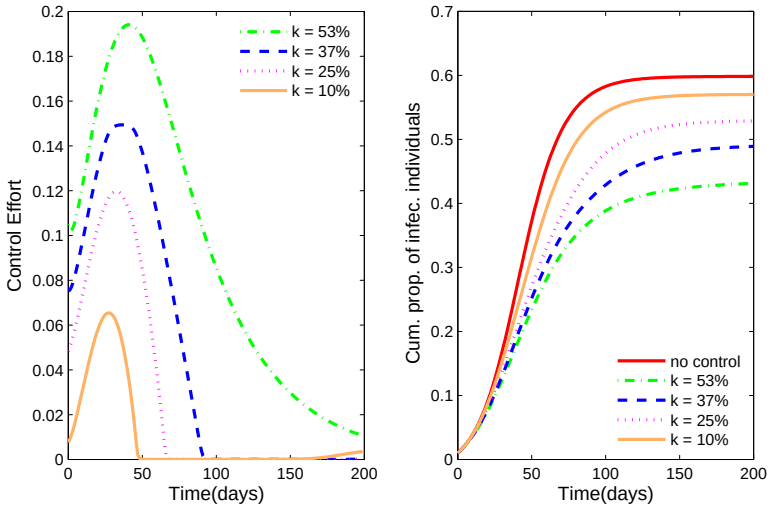

Figure 5.1: For $R_0 = 1.5$, the left figure shows the optimal control solution for different levels of treatment availability. For each value of k, the right figure shows that the final epidemic size is reduced by $28\%, 18\%, 12\%$, and 5%, respectively.

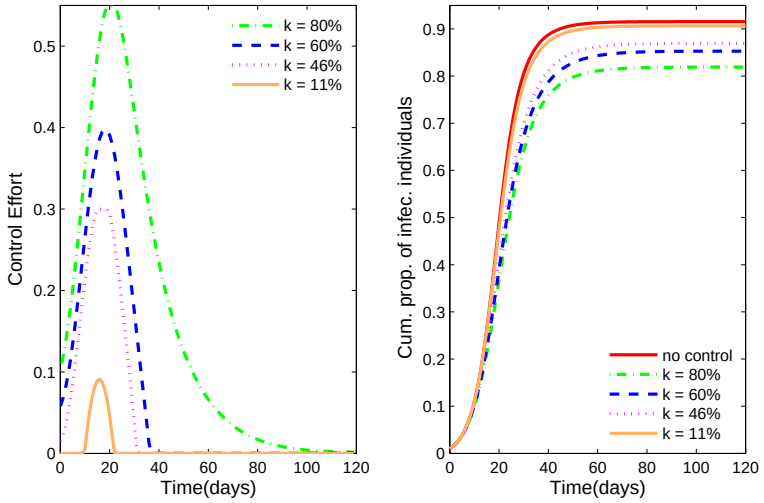

Figure 5.2: For $R_0 = 2.6$, the optimal control solution requires larger supplies of treatment than the ones for a small value of R_0. The final epidemic size is reduced by $11\%, 7\%, 5\%$, and 1% in each case.

5.3 Numerical Simulations: Two-Groups Model

In this section, we divide the population into two groups and assume that both groups have the same population size. We analyze the following three scenarios:

- Scenario 1: Same activity and susceptibility levels, i.e. $C_1 = C_2$ and $\rho_1 = \rho_2$.
- Scenario 2: Same activity level but Group 1 is more susceptible than Group 2, $\rho_1 > \rho_2$.
- Scenario 3: Same susceptibility but Group 1 is more active than Group 2, $C_1 > C_2$.

For each scenario, we assume a moderate value of R_0 (1.5-1.8). The final time of 180 days is chosen for all simulations. The baseline parameter values are given in Table 4.1. For each case, we present the proportion of infected individuals generated in the absence and presence of control strategies for different values of treatment doses k. Figures 5.3-5.5 show the optimal control function, the proportion of infected individuals, and the cumulative proportion of infected individuals in both groups under each scenario.

Scenario 1: Same Activity and Susceptibility Levels in Each Group

Since both groups have the same behavior, the treatment should be distributed equally for both populations (Figures 5.3A and 5.3D). Three values of k are used, by assuming that 4%, 7%, and 11% of the infected individuals get treatment; the final epidemic size is reduced by 4.5%, 8.1%, and 14.7% for each value of k, respectively. When resources are highly limited to 4% and 7%, Figures 5.3A and 5.3D show that the maximum amount of resources are used at the begining of the epidemic until all the resources are depleted (70 and 80 days, respectively).

Scenario 2: Same Activity Level, High Susceptibility in Group 1

Figure 5.4 shows the results for Scenario 2. The optimal control solution shows that more resources should be used for Group 1 (Figure 5.4A and 5.4C), since this is the high risk group; however the proportion of infected individuals is higher in Group 1 (Figures 5.4B and 5.4D). By using different values of k, 3%, 6%, and 13%, the final epidemic size in Group 1 is reduced by 2.4%, 6%, and 16% for each case; for Group 2, it is reduced by 3%, 7%, and

19%. Although the optimal solution allows the use of more resources towards Group 1, the reduction on the final epidemic size is a little higher in Group 2. For small values of k, (3% and 6%), Figures 5.4A and 5.4D show that in both groups, the resources should be used at the begining of the epidemic, 55 and 75 days respectively.

Scenario 3: Same Susceptibility, High Activity Level in Group 1

In the case of Scenario 3, Group 1 has a higher activity level than Group 2 but the same susceptibility. Figure 5.5 shows that the optimal control solution requires the application of more treatment doses in Group 1 (Figures 5.5A and 5.5D); however, the number of infected individuals is the same in both groups (Figures 5.5B and 5.5E). For different values of k ($4\%, 7\%$, and 14%), Figures 5.5C and 5.5E shows that the final epidemic size is reduced by $5\%, 8\%$, and 15% respectively.

In all scenarios, we find that the use of treatment reduces the number of infected individuals. In the case of two groups with the same population size and similar behavior, we get the same optimal control solution and therefore the same reduction on the final epidemic size. If one of the groups is more susceptible, more effort has to be implemented in that group, but the reduction in the final epidemic size will be larger in the less susceptible group. In addition, if we consider limited resources, we found that the resources should be used at the beginning of the epidemic until all the resources are used.

Summary of contribution: in this chapter, we included an isoperimetric constraint for the optimal control problem and solved it by using interior-point methods. Such constraints are used when the case of limited resources is considered. When Pontriagyn's Maximum Principle is applied, the problem has to be reformulated and the implementation of the forward-backward algorithm is not simple; We found that the use of interior-point methods make a big difference when this constraint is included. This methodology allowed to include the isoperimetric constraint in a very simple way. However since it is based on the Newton method, good initial conditions were required in order to guarantee convergence. We presented numerical results by considering one and two age groups. Our simulations showed

that the resources need to be used at the beginning of the epidemic until all the resources are exhausted.

In Chapters 3-5, we solved optimal control problems for different scenarios. We consider limited and unlimited resources and for seasonal and pandemic influenza. In the next chapter, we will address a different optimization problem: parameter estimation. In order to compare the model predictions with real data, it is necessary to estimate the parameter values for the model. Therefore, we will present two methodologies used to estimate parameters: Ordinary Least Squares (OLS) and Generalized Least Squares (GLS) [8, 9, 45]. We also present some applications of these techniques for discrete epidemiological problems.

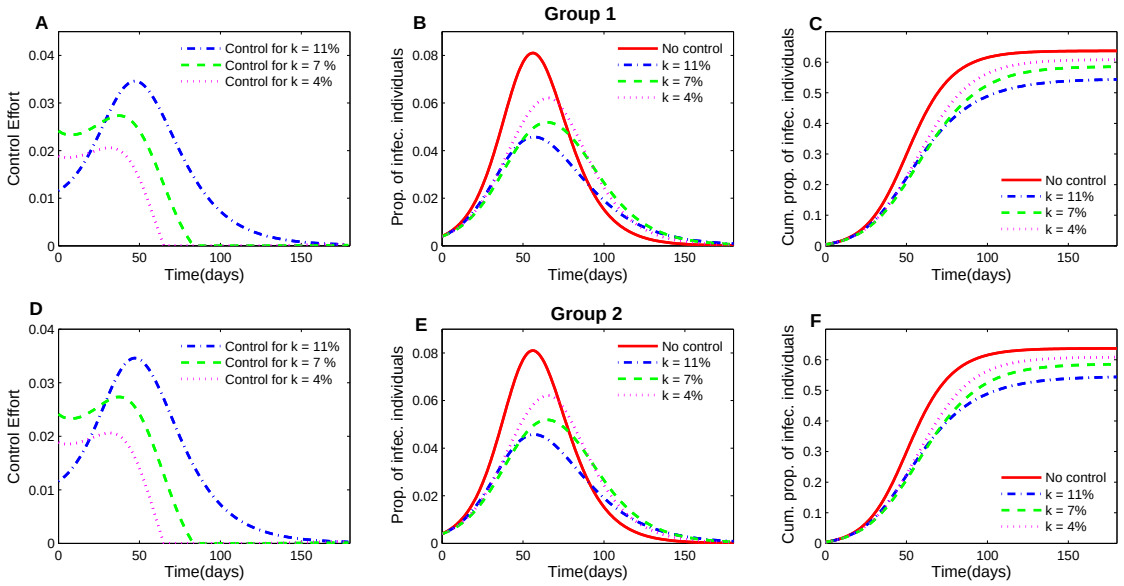

Figure 5.3: For Scenario 1, since both groups have similar behavior and same population size, the resources have to be distributed equally. Figures A and D show that in the case of very limited resources (4% and 7%), the largest amount of resources need to be used at the begining of the epidemic, until all the resources are exhausted.

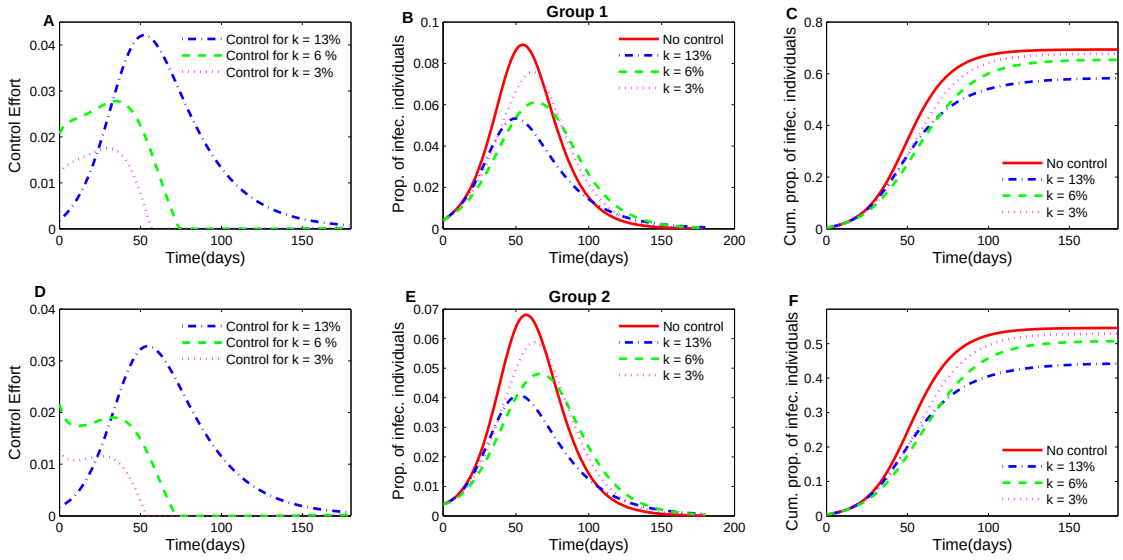

Figure 5.4: For Scenario 2, since Group 1 has higher activity level, more resources need to be used towards this group (Figure A and D) however for each value of k the reduction on the final epidemic size is higher in Group 2.

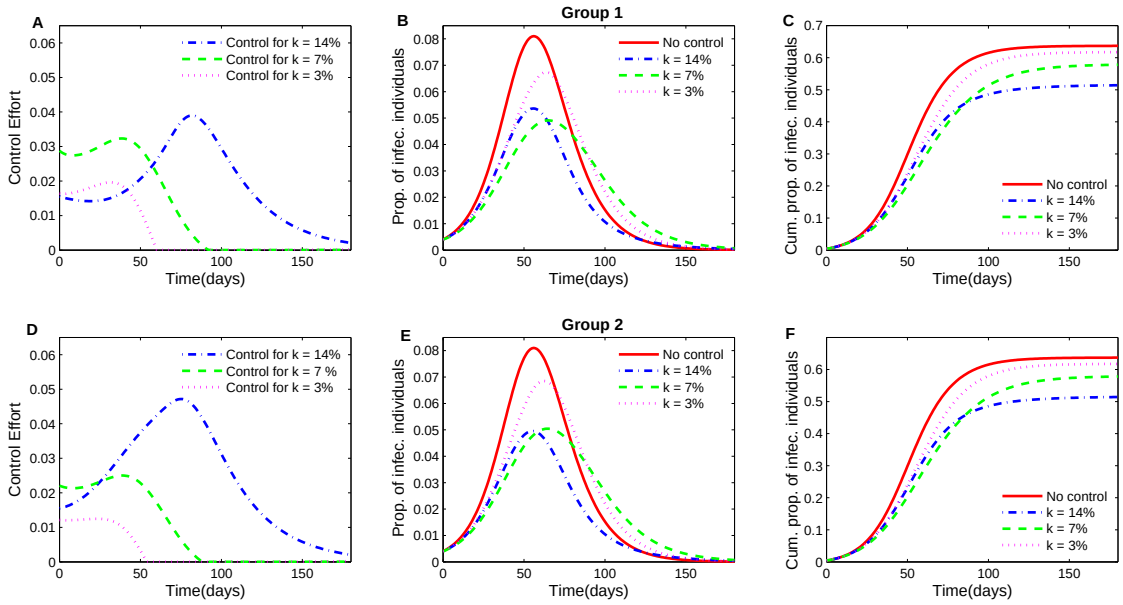

Figure 5.5: For Scenario 3, since Group 2 is at higher risk, more resources need to be used for this group. However, since the activity level is the same for both groups, the number of infected individuals is similar for Group 1 and Group 2.

Chapter 6

Parameter Estimation

6.1 Introduction

In the previous chapters, we considered optimal control problems on influenza dynamics for different scenarios; our goal was to find the best policy in order to minimize the number of infected individuals at the end of a single influenza outbreak. In this chapter, we present a different optimization problem: parameter estimation. This is important since epidemiological models contain parameters, such as contact rate, recovery rate, etc, these parameter values may be estimated in order to have a more realistic approach and to compare the model predictions with real data. The parameters in the model can be represented as a vector $\theta \in \mathbb{R}^m$, and the real data can be expressed as a vector $y \in \mathbb{R}^n$; therefore, a general parameter estimation problem can be written as:

$$F(\theta) = y. \tag{6.1}$$

In general, F is a non-linear function, and the number of parameters is smaller than the number of data, $m < d$. We need to find θ such as the model is consistent with the data in a best-fit sense [8]. Hence, our goal is to find an θ that minimize the residual value between the data and the theoretical predictions of the model. Parameter estimation for epidemiological models have been considered in [9, 14, 48, 49]. There are different methodologies to solve this kind of problems, we present Ordinary Least Squares (OLS) and Generalized Least Squares (GLS) techniques. In particular, we apply these techniques for three different discrete time epidemiological models. In Section 6.2, we estimate some parameters in a discrete SITR model by using synthetic data. We discuss the difference between constant and non-constant

variance noise in the data. In particular, we use residual plots to check if a correct statistical model has been specified or not [9]. In Section 6.3, we use both OLS and GLS to estimate parameters in a SIR model by using data from an influenza outbreak in a border school in United Kingdom; finally, we use data from the influenza pandemic in San Francisco (1918) and we estimate parameters by including asymptomatic individuals in Model (2.4).

6.2 Parameter Estimation for an SITR Model Using Synthetic Data

Here we present the problem formulation for both ordinary least squares and generalized least squares, along with experimental results from synthetic data. We consider a discrete time model where the total population is divided into susceptible (S), infectious (I), treated (T) and recovered (R) individuals. In this model, we assume that recovery occurs at the beginning of the stage, some infected individuals get treatment and some susceptible individuals get infected. We ignore the demographic change in the populations and we do not take into account disease-induced deaths. At time $t+1$, we assume that a fraction τ of the infectious individuals get treatment and its effective treatment rate is ρ. We assume that the fraction of susceptible individuals at time t that remain susceptible at time $t+1$ is given by [13]:

$$G_t = e^{-\beta \frac{I_t + \rho T_t}{N}},$$

where N denotes the total population. Let σ_1 and σ_2 be the probabilities of an infectious and treated individuals get recovered at time $t+1$. The model is given by the system of difference equations:

$$\begin{aligned} S_{t+1} &= S_t G_t \\ I_{t+1} &= S_t (1 - G_t) + (1 - \sigma_1)(1 - \tau) I_t \\ T_{t+1} &= (1 - \sigma_2) T_t + \tau (1 - \sigma_1) I_t \\ R_{t+1} &= R_t + \sigma_1 I_t + \sigma_2 T_t. \end{aligned} \tag{6.2}$$

Let us denote by $u = (S, I, T, R)$ and $\theta = (\beta, \rho)$, then our model (6.2) can be expressed as:

$$u_{t+1} = g(t, u_t, \theta).$$

From model (6.2) the cumulative number of infected individuals is given by:

$$f_i = I_0 + \sum_{i=1}^{n} S_{i-1} G_{i-1} \tag{6.3}$$

for $i = 1, 2, ..., n$, and $G_{i-1} = e^{-\beta \frac{I_{i-1} + \rho T_{i-1}}{N}}$. Using Model (6.2) and (6.3) we generate synthetic data using the parameter values given in Table 6.1 [43, 52]. Our goal is to estimate the effective contact rate β and the effective treatment rate ρ. We generate data according to two statistical models [9]:

$$Y_i = f(t_i, \theta_0) + \epsilon_j, \tag{6.4}$$

$$Y_i = f(t_i, \theta_0)(1 + \epsilon_j), \tag{6.5}$$

for $i = 1, 2, \ldots, n$. The components of θ_0 are the true values of the parameters used to generate the data, and ϵ_i are independent identically distributed random variables with $E(\epsilon_i) = 0$ and $var(\epsilon_i) = \sigma^2$.

In Model (6.4), the residuals are given by:

$$R_i = Y_i - f(t_i, \theta_0) = \epsilon_i; \tag{6.6}$$

we will refer to this term as the error with constant variance, denoted by CV. For (6.5) the residuals are given by:

$$R_i = Y_i - f(t_i, \theta_0) = \epsilon_i f(t_i, \theta_0) \tag{6.7}$$

i.e., are proportional to the model (6.3). Therefore we have error with non-constant variance, we will denote this case as NCV. We use both data sets with CV and NCV for estimating θ, using ordinary and generalized least squares techniques. We will discuss these techniques in the following subsection.

Table 6.1: Parameters used to generate synthetic data by using the SITR model (6.2)

parameter	description	value
β	effective contact rate	0.2909
ρ	effectiveness of treatment	0.6
τ	fraction of the infected individuals who get treatment	0.7
σ_1	recovered rate without treatment	1/7
σ_2	recovered rate with treatment	1/5

6.2.1 Ordinary Least Squares (OLS)

For the statistical model (6.4), let

$$\theta_{OLS} = \min \sum_{i=1}^{n} \left(Y_i - f(t_i, \theta_0)\right). \tag{6.8}$$

Notice that solving problem (6.8) is equivalent to solving:

$$\sum_{i=1}^{n} \left[\left(Y_i - f(t_i, \theta_0)\right) \nabla f(t_i, \theta_0)\right] = 0. \tag{6.9}$$

By using the Gauss-Newton method [45], let $R_i = Y_i - f(t_i, \theta_0)$ and J be the Jacobian of f; the procedure to solve the problem (6.8) is summarized in Algorithm 3:

Algorithm 3 OLS Algorithm

1: Given an initial point θ_{init}.

2: **for** $k = 0, 1, 2 \ldots$ until convergence **do**

3: Gauss - Newton step

$$J_k^T J_k \Delta\theta = -J_k^T R_k$$

4: Update $\theta = \theta + \Delta\theta$.

5: Check convergence, if $||J_k^T R_k|| < \epsilon$, break,

6: **end for**

Different initial conditions are selected randomly; the results by using these initial conditions for constant and non-constant variance, are given in Tables 6.2 and 6.3.

Table 6.2: Parameter estimation using ordinary least squares and constant variance data, with 5% of noise and $(\beta_{true}, \rho_{true}) = (0.2909, 0.6)$

Starting Point (β_0, ρ_0)	(β^*, ρ^*)	$\|\nabla f\|$	# of iterations
(0.5687,0.3058)	$(0.2914, 0.5983)$	1.79×10^{-8}	5
(0.1190,0.3134)	$(0.2914, 0.5983)$	4.48×10^{-8}	5
(0.3864,0.5025)	$(0.2914, 0.5983)$	1.79×10^{-8}	5
(0.0325,0.0531)	$(0.2914, 0.5983)$	1.44×10^{-7}	7
(0.7115,0.3649)	$(0.2914, 0.5983)$	2.70×10^{-8}	5

Table 6.3: Parameter estimation using ordinary least squares and non-constant variance data, with 5% of noise and $(\beta_{true}, \rho_{true}) = (0.2909, 0.6)$

Starting Point (β_0, ρ_0)	(β^*, ρ^*)	$\|\nabla f\|$	# of iterations
$(0.1758, 0.3157)$	$(0.2707, 0.6695)$	1.11×10^{-8}	5
$(0.5462, 0.3595)$	$(0.2707, 0.6695)$	2.53×10^{-7}	5
$(0.4327, 0.1577)$	$(0.2707, 0.6695)$	1.46×10^{-7}	5
$(0.4095, 0.4288)$	$(0.2707, 0.6695)$	1.14×10^{-7}	5
$(0.4600, 0.5682)$	$(0.2707, 0.6695)$	6.39×10^{-8}	5

We found that for 5% of noise, by using different initial conditions we get the estimates $\beta = 0.291406$, and $\rho = 0.598297$ for constant variance; we get $\beta = 0.270727$ and $\rho = 0.669467$ for non-constant variance. In Section 6.2.3, we present the residual test; this test helps to determine if the assumptions and the method were right.

6.2.2 Generalized Least Squares (GLS)

By using the statistical model (6.5), $E(\epsilon_i) = f(t_i, \theta_0)$ and $var(\epsilon_i) = \sigma^2 f^2(t_i, \theta_0)$; in this case the variance depends upon the model f. Therefore, we use the generalized least square (GLS) to estimate θ [9, 14]. We need to solve the equation:

$$\sum_{i=1}^{n} w_i \left(Y_i - f(t_i, \theta_{GLS})\right) \nabla f(t_i, \theta_{GLS}) = 0, \tag{6.10}$$

where Y_i is given by (6.5) and $w_i = f^{-2}(t_i, \theta_{GLS})$ [9]. For solving (6.10) we also use the Gauss-Newton method. Let be $W = diag(w_1, w_2, \ldots, w_n)$ then by changing Step 3 in Algorithm 3, we obtain the GLS Algorithm 4:

Algorithm 4 GLS Algorithm

1: Given an initial point θ_{init}.

2: **for** $k = 1, 2, \ldots$ until convergence **do**

3: Gauss-Newton step

$$J_k^T W_k J_k \Delta\theta = -J_k^T W_k R_k.$$

4: Update $\theta = \theta + \Delta\theta$.

5: Check convergence; if $||J_k^T W_k R_k|| < \epsilon$, break.

6: **end for**

We use 5% of noise with different initial conditions and GLS method. We obtain $\beta = 0.297121$ and $\rho = 0.579450$ for constant variance, and $\beta = 0.296562$, $\rho = 0.580681$ for non-constant variance. The results of selected simulations are given in Table 6.4 and Table 6.5.

In general, we do not know the form of error in the data and therefore, we do not which method we should use, OLS or GLS. For this reason, we need to investigate our statistical assumptions to determine if we chose the correct one; for this purpose, we use a residual test [9]: we plot residual vs. time and residual vs. model to determine if our assumptions are correct. In Section 6.2.3, we present this test.

Table 6.4: Parameter estimation using generalized least squares and constant variance data, with 5% of noise and $(\beta_{true}, \rho_{true}) = (0.2909, 0.6)$

Starting Point (β_0, ρ_0)	(β^*, ρ^*)	$\|\nabla f\|$	# of iterations
$(0.5687, 0.3058)$	$(0.2971, 0.5795)$	8.46×10^{-8}	5
$(0.1190, 0.3134)$	$(0.2971, 0.5795)$	5.54×10^{-8}	6
$(0.3864, 0.5025)$	$(0.2971, 0.5795)$	1.85×10^{-9}	5
$(0.0325, 0.0531)$	$(0.2971, 0.5795)$	1.55×10^{-7}	7
$(0.7115, 0.3649)$	$(0.2971, 0.5795)$	9.27×10^{-7}	5

Table 6.5: Parameter estimation using generalized least squares and non-constant variance data, with 5% of noise and $(\beta_{true}, \rho_{true}) = (0.2909, 0.6)$

Starting Point (β_0, ρ_0)	(β^*, ρ^*)	$\|\nabla f\|$	# of iterations
$(0.1758, 0.3157)$	$(0.2966, 0.5807)$	4.53×10^{-8}	6
$(0.5462, 0.3595)$	$(0.2966, 0.5807)$	6.53×10^{-8}	6
$(0.4327, 0.1577)$	$(0.2966, 0.5807)$	2.54×10^{-7}	6
$(0.4971, 0.2078)$	$(0.2966, 0.5807)$	2.37×10^{-7}	6
$(0.4095, 0.4288)$	$(0.2966, 0.5807)$	2.52×10^{-8}	6

6.2.3 Residual Test

We use the residuals in order to check whether our assumptions are correct. For OLS, we plot residuals vs. model and residuals vs. time [9]. For constant variance, we have, from equation (6.6):

$$R_i = Y_i - f(t_i, \theta_0) = \epsilon_i;$$

since the residuals do not depend upon the model, we obtain a random plot. If the data is incorrectly assumed, to be CV, and we use OLS in a non-constant variance data set, we obtain a pattern, because the residuals depend of the model (6.7), i.e.,

$$R_i = Y_i - f(t_i, \theta_0) = \epsilon_i f(t_i, \theta_0).$$

Figures 6.1 and 6.2 show residual vs model and residuals vs time using Algorithm 3. Notice that we obtain a random plot in Figure 6.1, because the residuals do not depend upon the model. However, Figure 6.2 shows a pattern, which means that the assumptions is not correct, and thus, OLS should not be used since we have non-constant variance.

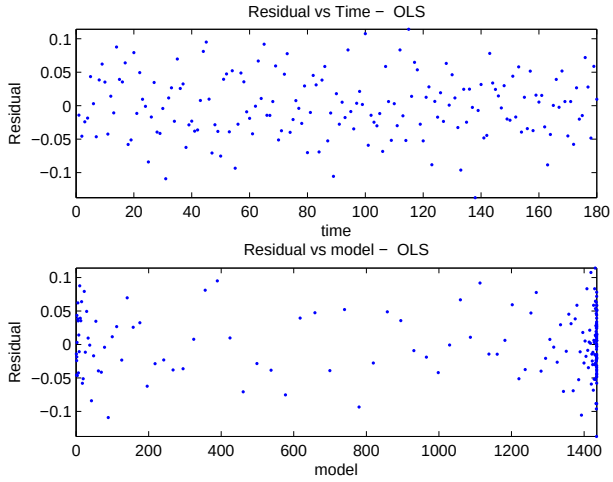

Figure 6.1: Residual vs. time and residual vs. model plots with 5% of noise, using OLS and constant variance. Since the data is correct assumed we get a random pattern.

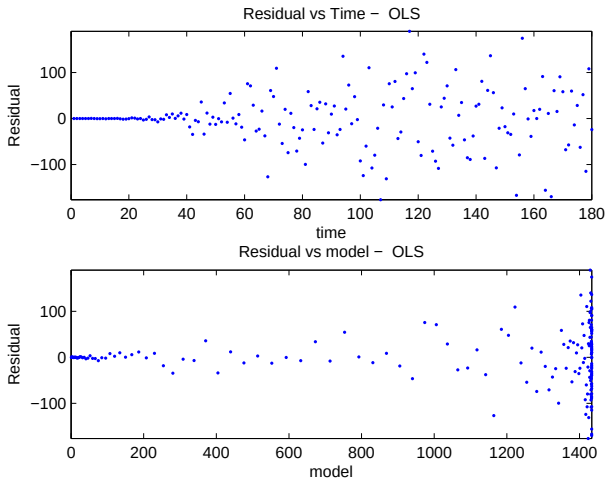

Figure 6.2: Residual vs. time and residual vs. model plots with 5% of noise, using OLS and non-constant variance. Since the assumption is not correct, we observe a pattern.

For non-constant variance data, we modify the residuals; let

$$R_{mod} = \frac{Y_i - f(t_i, \theta_0)}{f(t_i, \theta_0)} = \epsilon_i;$$

notice that the modified residuals do not depend on the model. Hence for GLS, if we plot R_{mod} vs. model and R_{mod} vs. time we obtain a random plot.

When we use GLS, we plot the modified residuals vs. model and the modified residuals vs. time; Figure 6.4 shows a pattern when we have non-constant variance, because this plot is based on wrong assumptions. On the other hand, Figure 6.5 shows a random plot; this means that the assumption is correct: for non-constant variance, the modified residuals do not depend on the model, and we obtain a random plot.

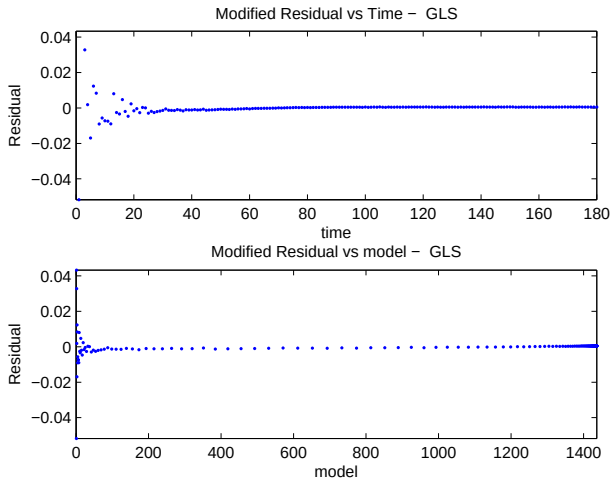

Figure 6.3: Modified residual vs. time and modified residual vs. model plots with 5% of noise, using GLS and constant variance. Since the assumption is not correct, we get a pattern.

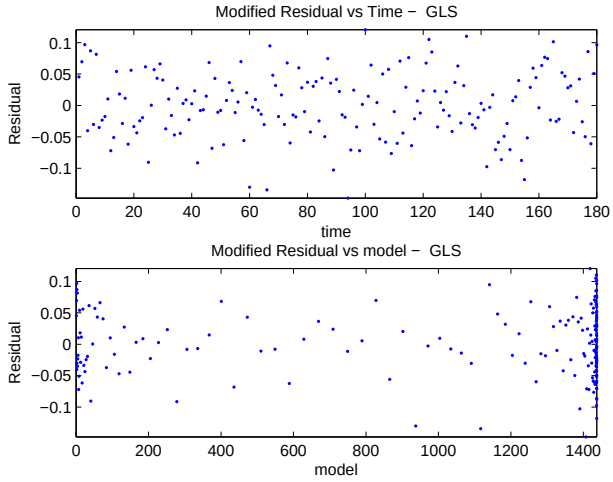

Figure 6.4: Modified residual vs. time and modified residual vs. model plots with 5% of noise, using GLS and non-constant variance. Since the assumption is correct, we get a random plot.

In what follows, we solve the parameter estimation problem for real data. We describe and report our experiments using Ordinary Least Squares and Generalized Least Squares

by using data from a border school in the United Kingdom and from the 1918 influenza pandemic in San Francisco.

6.3 Parameter Estimation for Real Data

6.3.1 Influenza Outbreak in a Border School, United Kingdom

In 1978 an influenza outbreak was reported in a border school in the United Kingdom; the number of infected individuals was recorded daily [20]. We use a discrete SIR model to describe this outbreak. The model is a simplified version of Model (6.2), when treatment is not available. The SIR model is given by the system of difference equations:

$$\begin{aligned} S_{t+1} &= S_t G_t \\ I_{t+1} &= S_t\,(1 - G_t) + (1 - \sigma)\, I_t \\ R_{t+1} &= R_t + \sigma I_t, \end{aligned} \tag{6.11}$$

where

$$G_t = e^{-\beta \frac{I_t}{N}}. \tag{6.12}$$

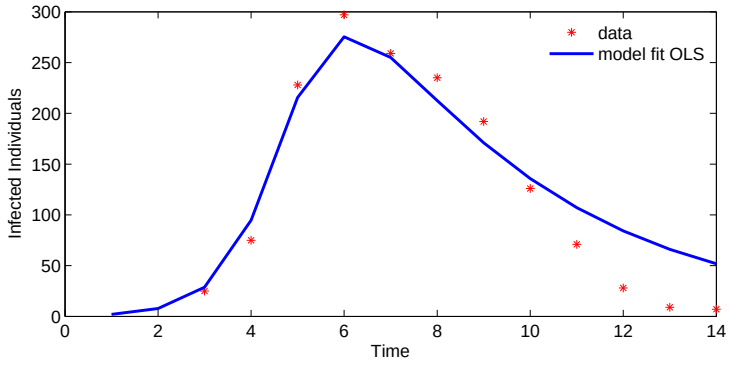

Figure 6.5: The solution using OLS was reached in 34 iterations. The estimate parameters are $\beta = 3.1238$ and $\sigma = 0.2192$.

The total population (N) is 763 individuals, and the final time is 14 days. By using OLS and GLS methods introduced in the previous section, we estimate the susceptibility (β) and

the probability that an infectious individual get recovered (σ), where the function f is given by the daily number of infected individuals, From model (6.11):

$$f_i = S_i\,(1 - G_i) + (1 - \sigma)\,I_i \tag{6.13}$$

for $i = 1, 2, ..., n$, with G_i given by 6.12.

Figure 6.5 shows the data and model fit by using OLS. The estimate values are $\beta = 3.1238$ and $\sigma = 0.2192$. The solution was reached in 36 iterations when the initial values are $\beta_0 = 2.1$ and $\sigma_0 = 0.15$. The solution does not depend on the initial conditions, by changing the values of β_0 and σ_0 we get the same solution in a different number of iterations.

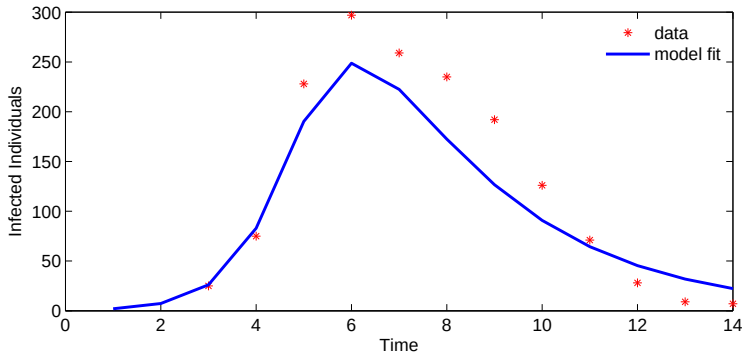

Figure 6.6: Model fit using GLS. The estimate for parameters are $\beta = 3.0306$ and $\sigma = 0.3154$.

By using GLS, the estimate for parameters are $\beta = 3.0306$ and $\sigma = 0.3154$; the solution was reached in 25 iterations, for $\beta_0 = 2.1$ and $\sigma_0 = 0.15$ as initial values.

As in the previous section we tried to apply the residual test, but the results did not lead to a definite conclusion. Therefore, as an estimate we take an average of the values that we obtain by using OLS and GLS; hence, we conclude that $\beta = 3.0771 \pm 0.1429$ and $\sigma = 0.27 \pm 0.05$. Figure 6.7 shows the data and model fit for the averages values.

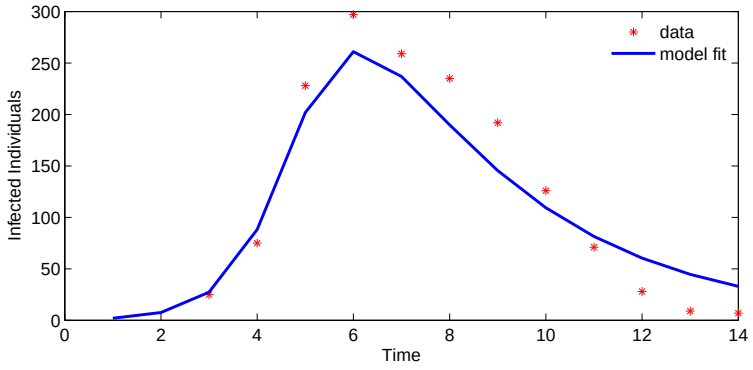

Figure 6.7: Model fit by using the average values, $\beta = 3.0771$ and $\sigma = 0.27$.

6.3.2 Influenza Pandemic in San Francisco (1918)

In this section, we use data from the influenza pandemic in San Francisco (1918). This pandemic, also known as the Spanish Flu, is the most severe pandemic in recent history [22, 23]. To describe this pandemic, we modify Model (2.4) introduced in Chapter 2. We assume that a fraction q of the infected individuals does not get symptoms, so we include a class A of asymptomatic individuals. We present an optimal control problem considering asymptomatic individuals in [37]. We assume that asymptomatic individuals are still infectious, but there is an infectiousness reduction m. Since both treated and asymptomatic individuals are infectious, we modify the expression (2.3) as follows:

$$G_t = \rho \frac{I_t + \epsilon T_t + m A_t}{N_t}; \tag{6.14}$$

the model is given by the system of difference equations:

$$\begin{aligned} S_{t+1} &= S_t(1 - G_t) \\ A_{t+1} &= qS_tG_t + (1 - \sigma_1)(1 - \delta)A_t \\ I_{t+1} &= (1 - q)S_tG_t + (1 - \tau_t)(1 - \sigma_1)(1 - \delta)I_t \\ T_{t+1} &= (1 - \sigma_2)T_t + \tau_t(1 - \sigma_1)(1 - \delta)I_t \\ R_{t+1} &= R_t + \sigma_1(1 - \delta)I_t + \sigma_1(1 - \delta)A_t + \sigma_2 T_t. \end{aligned} \tag{6.15}$$

We assume that 35% of the infected individuals get treatment and $q = 92\%$ of the infected individuals are asymptomatic with an infectiouness reduction of $m = 0.5$. The mortality due

to the disease is given by $\delta = 0.03$, the values for the recovery with and without treatment (σ_2 and σ_1) are given by $\frac{1}{7}$ and 0.2 respectively. Our goal is to estimate the susceptibility ρ and the effectiveness of the treatment ϵ. By using OLS, we do not get convergence, hence we solve the problem by using GLS; however, we had to modify Algorithm 4 in order to get a solution. In Step 3, we change the W matrix by $W = \text{diag}(\hat{w}_i)$ where $\hat{w}_i = \frac{1}{\hat{f}_i^2 + \|R\|^2}$ and R is given by (6.6). In this case, the function f is given by the incidence (number of new cases per day). From Model (6.15), the incidence is given by:

$$f_i = (1 - q)S_t G_t \tag{6.16}$$

for $i = 1, 2, ..., n$, and G_t given by (6.14).

Figure 6.8 shows the data and model fit for estimated values of $\rho = 0.8996$ and $\epsilon = 0.9115$; the solution was reached in 4 iterations.

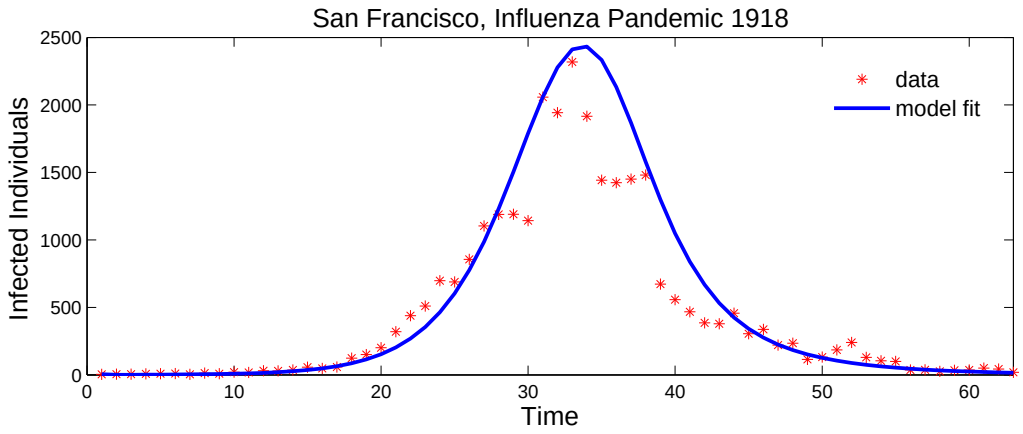

Figure 6.8: Model fit by using GLS. The solution was reached in 4 iterations

Summary of Contribution: the problem of parameter estimation was addressed in this chapter. Two methodologies were presented: Ordinary Least Squares and Generalized Least Squares. These techniques have been widely used, in particular, for continuous time epidemiological models [9, 48, 49]. Our main contribution in this chapter was to adjust the methodology presented in [9] for a discrete time epidemiological model by using synthetic data. In addition, we used a discrete time model to estimate data from a influenza outbreak

in a border school in United Kingdom. A similar problem was solved by using a continuous time model [13]. Our findings were similar to the ones in the continuous case; however, we found that a discrete formulation allows us to solve the parameter estimation problem in a simpler way. Finally, we estimated parameters by using data from the influenza pandemic in San Francisco (1918); for this particular problem, we introduced a class of asymptomatic individuals in our original problem and we formulate a different matrix W for the generalized least squares method. Because of convergence issues, we confined ourselves to estimate the values of the susceptibility ρ and the effectiveness of the treatment ϵ. As future work, we want to estimate the fraction of individuals that do not get symptoms q and the infectiousness reduction of the asymptomatic individuals m.

Chapter 7

Conclusion and Future Work

7.1 Conclusion

We presented a novel discrete time model in order to study single epidemic outbreaks in the context of influenza. In this model, individuals were classified as susceptible, infected, treated, or recovered. We formulated an optimal control problem in order to minimize the number of infected individuals by using the least amount of resources for treatment and social distancing. We compared three different strategies: social distancing, treatment, and a combination of both mitigation strategies.

The problem was solved by using two techniques: the forward-backward algorithm and primal-dual interior-point method. The first method has been used on many applications, in particular for optimal control problems in epidemiology. The second method has become a popular choice for solving large scale constrained optimization problems. The numerical advantages, first demonstrated in the seminal work of Karmarkar [35], have led interior-point methodologies to be implemented in a variety of applications in fields like economics, machine learning, medical imaging, and geophysics. To our knowledge, it has not been previously used to solve control problems in epidemiology. Our numerical results showed that the primal-dual interior-point method reached the solution with fewer iterations and with a competitive function value at the solution when compared to the forward-backward algorithm.

We found that the use of single and dual strategies (social distancing and antiviral treatment) resulted in increased reductions on the cumulative number of infected individuals. Our results confirm the general expectation that dual strategies are more efficient at reducing the

final epidemic size than single policies. Our results showed that under the implementation of a single policy, the social distancing strategy (Strategy 1) was more effective than the antiviral treatment strategy (Strategy 2) when the basic reproductive number R_0 (the number of secondary cases produced by a single infected individual in a population of susceptible individuals) is greater than 1.4. Some of these results have been published in [37, 38].

Moreover, we extended our model to a group-structured model under the assumption that people mix more with individuals in the same group and groups are mixing randomly. We introduced an optimal control problem (4.7) in order to study how control policies should be implemented in each group; our goal was to minimize the number of infected individuals. Because of the introduction of groups into the model, the problem became computationally more expensive; thus we solved it by using the primal-dual interior-point method. We analyzed different scenarios by considering both seasonal and pandemic influenza in the case of two or three age-groups. Our numerical results showed that the implementation of policies should be adjusted according to the characteristics associated with a newly emerged virus; for example, it will be necessary to determine which group is the more susceptible. In all scenarios, we found that the implementation of policies reduced the number of infected individuals. The results were sensitive to the population size; for example, more resources were needed for larger-size population groups and groups with higher activity level.

In addition, we considered the case of limited resources by including an isoperimetric constraint (5.1). A continuous influenza model with limited supplies was studied in [40]. The continuous problem, considered in [40] was solved by using the Pontryagin's Maximum Principle. However, with that formulation, convergence issues need to be addressed because of the inclusion of the new constraint. We solved this problem by using the primal-dual interior-point method, since for this method the inclusion of the new constraint is simpler. We found that the solution was very sensitive to initial conditions; because this technique is based on the Newton's Method, thus good initial conditions were required in order to guarantee convergence.

Finally, we addressed the parameter estimation problem. In real life problems, the pa-

rameter values in a epidemiological model should be estimated in order to compare the model predictions with real data. Two techniques were presented and applied to discrete epidemiological models: Ordinary Least Squares and Generalized Least Squares. Following the ideas presented in [9] for a continuous model, we generated synthetic data by using a discrete SITR model; parameters were estimated and the residual test was applied to this data set. We also estimated parameters by using data for an influenza outbreak in a border school in the United Kingdom and from the 1918 influenza pandemic in San Francisco.

7.2 Future Work

For the optimal control problem we would like to improve our algorithm; we want to use a better globalization strategy in order to have a solution with less sensitivity to initial conditions. In our simulations, the values of the weight constants in the objective function are selected, in part, to facilitate computational issues; we claim that by improving the algorithm, more realistic values for the weight constants can be used. In particular, we compared the numerical results obtained by our algorithm, and those obtained by a professional solver, e.g., KNITRO [44]. We found out that our results are competitive in terms of accuracy and efficiency. In general, our implementation of interior point methods appears to be more efficient; this is probably due to our globalization strategy, but the professional software we also used to compare is more robust since its performance is more independent from the initial condition and weight constants' choices. Further work can be done to improve the performance of our algorithm, but this is beyond the scope of this work. In addition, by using an improved algorithm, we could address a more realistic epidemiological model, for example we could include more epidemic classes, as asymptomatic individuals, and more age-group classes in the model.

In the case of the parameter estimation problem, we will like to improve the algorithm in order to estimate more parameter values in the model. In particular, for the problem using data from the influenza pandemic in San Francisco, we estimated the values of the

susceptibility ρ and the effectiveness of the treatment ϵ. We want to estimate the fraction of individuals that do not get symptoms q and the infectiousness reduction of the asymptomatic individuals m; because of convergence issues, we were not able to estimate this values.

References

[1] L.J. Allen and A.M. Burgin, "Comparison of Deterministic and Stochastic SIS and SIR Models in Discrete Time," *Math. Biosci.*, 2000, Vol. 163, pp. 1–33.

[2] L.J. Allen and P. van den Driessche, "The Basic Reproductive Number in Some Discrete Time Epidemic Models," *Journal of difference equations and applications*, 2008, Vol. 14, No. 10-11, pp. 1127–1147.

[3] R.M. Anderson and R.M. May, *Infectious Diseases of Humans: Dynamics and Control*, Oxford University Press, Oxford, UK, 1992.

[4] S. Anita, V. Arnautu and V. Capasso, *An Introduction to Optimal Control Problems in Life Sciences and Economics*, Birhauser, 2010.

[5] M. Argaez, and R. Tapia, "On the Global Convergence of a Modified Augmented Lagrangian Interior-Point Newton Method for Nonlinear Programming." *Journal of Optimization Theory and Applications*, 2002, Vol. 114, pp. 1–25.

[6] M. Argaez, R. Tapia, and L. Velazquez. "Numerical Comparisons of Path-Following Strategies for a Primal-Dual Interior-Point Method for Nonlinear Programming." *Journal of Optimization Theory and Applications*, 2002, Vol. 114, No. 2.

[7] J. Arino, F. Brauer, P. van den Driessche, J. Watmough, and J. Wu, "A Model for Influenza with Vaccination and Antiviral Treatment," *J. Theor. Biol.*, 2003, Vol. 253, pp. 118–130.

[8] R.C. Aster, B. Borchers, and C.H. Thurber, *Parameter Estimation and Inverse Problems*, Elsevier, 2005.

[9] T. Banks, M. Davidian, J. Samuels Jr and K. Sutton, "An Inverse Problem Statistical Methodology Summary" *Mathematical and Statistical Estimation Approaches in Epidemiology*. 2009.

[10] H. Behncke, "Optimal Control of Deterministic Epidemics," *Opt. Control Appl. Meth.*, 2000, Vol. 21, pp. 269–285.

[11] F. Brauer and C. Castillo-Chavez, *Mathematical Models in Population Biology and Epidemiology*, Springer-Verlag, 2010.

[12] F. Brauer, "Epidemic Models with Heterogeneous Mixing and Treatment," *Bulletin of Mathematical Biology*, 2008, Vol. 70, pp. 1869–1885.

[13] F. Brauer, Z. Feng, and C. Castillo-Chavez, "Discrete Epidemic Models," *Math. Biosc. & Eng.*, 2010, Vol. 7, pp. 1–15.

[14] A. Cintron-Arias, C. Castillo-Chavez, L.M.A. Bettencourt, A.L. Lloyd, and H.T. Banks, "The Estimation of the Effective Reproductive Number From Disease Outbreak Data," *Math. Biosc. & Eng.*, 2009, Vol. 6, No. 2, pp. 261-282.

[15] C. Castillo-Chavez and A-A. Yakubu, "Discrete-time S-I-S models with Complex Dynamics," *Nonlinear Analysis*, 2001, Vol. 47, pp. 4753–4762.

[16] C. Castillo-Chavez and A-A. Yakubu, "Discrete-time S-I-S Models with Simple and Complex Population Dynamics," *Mathematical Approaches for Emerging and Reemerging Infectious Diseases*, (eds., C. Castillo-Chavez, et al.), Springer-Verlag, IMA, 2001, Vol. 125, pp. 153–163.

[17] C. Castillo-Chavez and H.W Hethcote, "Epidemiological Models with Age Structure, Proportionate Mixing, and Cross Immunity." *Journal of mathematical biology*, 1989, Vol. 27, pp. 233–258.

[18] 2009 H1N1 Flu. Center for Disease Control and Prevention. http://www.cdc.gov/h1n1flu/pdf/graph_April202010N.pdf April 2010.

[19] http://who.int/mediacentre/news/statements/2009/h1n1_pandemic_phase6_20090611/en/index.html, 11 Jun. 2009.

[20] Communicable Disease Surveillance Centre, "Influenza in a Boarding School." *British Medical Journal*, 1978, Vol 1.

[21] M. Chan, "World Now at the Start of 2009 Influenza Pandemic", http://who.int/mediacentre/news/statements/2009/h1n1_pandemic_phase6_20090611/en/index.html, 11 Jun. 2009.

[22] G. Chowell, C.E. Ammon, N.W. Hengartner, and J.M. Hyman, "Transmission Dynamics of the Great Influenza Pandemic of 1918 in Geneva, Switzerland: Assessing the Effects of Hypothetical Interventions," *J. Theor. Biol.*, 2006, Vol. 241, pp. 193–204.

[23] G. Chowell, N.W. Hengartner, C. Ammon, and J.M. Hyman, "Learning From the Past to Prepare for the Future: Modeling the Impact of Hypothetical Interventions During the Great Influenza Pandemic of 1918," *CHANCE*, Springer New York, 2008, Vol. 21, pp. 55–60.

[24] S.Y Del Valle, J.M Hyman, H.W Hethcote, and S.G. Eubank. "Mixing Patterns between Age Groups in Social Networks." *Social Networks*, 2007. Vol. 29, pp. 539-554.

[25] W. Ding, L. Gross, K. Langston, S. Lenhart, and L. Real, "Rabies in Racoons: Optimal Control for a Discrete Time Model on a Spatial Grid", *J. Biol. Dynamics*, 2007, Vol. 1, pp. 307–393.

[26] A.S. El-Bakry, R.A. Tapia, T. Tsuchiya, and Y. Zhang. "On the Formulation and Theory of the Primal-Dual Newton Interior-Point Method for Nonlinear Programming," *Journal of Optimization Theory and Applications*. 1996. Vol. 89, No. 3, pp. 507–541.

[27] E. Fenichel, C. Castillo-Chavez, P. Gonzalez-Parra, et al, "Adaptive human behavior in epidemiological models," *Proceeding of the National Academy of Sciences PNAS*, 2011, Vol. 108, No. 15.

[28] W.H. Fleming and R.W. Rishel. *Deterministic and Stochastic Optimal Control*, Springer Verlag. 1975.

[29] H.W. Hethcote, "The Mathematics of Infectious Diseases," *SIAM Rev*, 2000, Vol. 42, pp. 599–653.

[30] H.W. Hethcote. "An Age-Structured Model for Pertusis Transmission." *Mathematical Biosciences*. 1997. Vol. 145, pp. 89–136.

[31] M.A. Herrera-Valdez, M. Cruz-Aponte and C. Castillo-Chavez, "Multiple Outbreaks for the Same Pandemic: Local Transportation and Social Distancing Explain the Different "Waves" of A-H1N1pdm Cases Observed in Mxico During 2009," *Math. Biosc.* & *Eng.*, 2011, Vol. 8, pp. 21–48.

[32] R. Hilschera and V. Zeidanb, "Discrete Optimal Control: The Accessory Problem and Necessary Optimality Conditions," *Journal of Mathematical Analysis and Applications*, 2000, Vol. 243, pp. 429–452.

[33] C. Hwang and L. Fan, "A Discrete Version of Pontryagin's Maximum Principle," *Operations Research*, 1967, Vol. 15, pp. 139–146.

[34] E. Jung, S. Lenhart, V. Protopopescu, and C.F. Babbs, "Optimal Control Theory Applied to a Difference Equation Model for Cardiopulmonary Resuscitation," *Mathematical Models and methods in Applied Sciences*, 2005, Vol. 15, pp. 1519–1531.

[35] N. Karmarkar, "A New Polynomial Time Algorithm for Linear Programming," *Combinatorica*, 1984, Vol. 4, pp. 373–395.

[36] W.O. Kermack and A.G. McKendrick, "A Contribution to the Mathematical Theory of Epidemics," *Proc. R. Soc. London*, 1927, Vol.115, pp. 700-721.

[37] P. González-Parra, S. Lee, L. Velazquez, and C. Castillo-Chavez, "A Note on the Use of Optimal Control on a Discrete Time Model of Influenza Dynamics." *Math. Biosc. & Eng.*, 2011, Vol. 8, No. 8, pp. 183–197.

[38] P. González-Parra, L. Velazquez, M.C. Villalobos and C. Castillo-Chavez, "Optimal control applied to a discrete influenza model." *Conference Proceedings Book of the XXXVI International Operation Research Applied to Health Services*, 2010.

[39] S. Lee, G. Chowell, and C. Castillo-Chavez, "Optimal Control for Pandemic Influenza: the Role of Limited Antiviral Treatment and Isolation," *J.Theor. Biol.*, 2010, Vol. 265, pp. 136–150.

[40] S. Lee, R. Morales, and C. Castillo-Chavez, "A Note on the Use of Influenza Vaccination Strategies when Supply is Limited," *Math. Biosc. & Eng.*, 2011, Vol. 8, pp. 171–182.

[41] S. Lee, M. Golinski, and G. Chowell, "Modeling Optimal Age-Specific Vaccination Strategies Against Pandemic Influenza," *Bulletin of Mathematical Biology*, 2011.

[42] S. Lenhart and J. Workman, *Optimal Control Applied to Biological Models*, Chapman & Hall, CRC Mathematical and Computational Biology series, 2007.

[43] H. Nishiura,C. Castillo-Chavez, M. Safan, and G. Chowell, "Transmission Potential of the New Influenza A(H1N1) Virus and its Age-specificity in Japan." *Eurosurveillance,* 2009, Vol. 14, Issue 22.

[44] J. Nocedal, KNITRO: `http://www.ziena.com/knitromatlab.htm`

[45] J. Nocedal and S.J. Wright, *Numerical Optimization*, 2nd Edition. Springer Verlag. 2006.

[46] M. Nuno, G. Chowell, X. Wang, and C. Castillo-Chavez, "On the Role of Cross-immunity and Vaccines on the Survival of Less Fit Flu-strains", *Theor. Pop. Biol.*, Elsevier, 2007, Vol. 71, pp. 20–29.

[47] L.S. Pontryagin, V. Boltyanskii, R. Gamkrelidze, and E. Mishchenko, *The Mathematical Theory of Optimal Processes*, Wiley, New Jersey, 1962.

[48] K.L. Sutton, H.T. Banks, C. Castillo-Chavez "Using Inverse Problem Methods with Surveillance Data in Pneumococcal Vaccination." *Math Computational Modeling*, 2010, Vol. 51, pp. 369–388

[49] K.L. Sutton, H.T. Banks, C. Castillo-Chavez "Estimation of invasive pneumococcal disease dynamics parameters and the impact of conjugate vaccination in Australia." *Mathematical Biosciences and Engineering*, 2008, Vol. 5, pp. 175–204

[50] J.M. Tchuenche, S.A. Kamis, F.B. Agusto, and S.C. Mpesche, "Optimal Control and Sensitivity Analysis of an Influenza Model with Treatment and Vaccination," *Acta Biotheoretica*, Springer, 2011, Vol. 59, No. 1, pp. 1–28.

[51] S.M. Tracht, S. Del Valle, and J. Hyman, "Mathematical Modeling of the Effectiveness of Facemasks in Reducing the Spread of Novel Influenza A (H1N1)" *PLoS ONE*, 2010, www.plosone.org, Vol. 5.

[52] A. Tuite, A. Greer et al, "Estimated Epidemiologic Parameters and Morbidity Associated with Pandemic H1N1 Influenza," *Can. Med. Assoc. Journal*, 2010, Vol. 182, pp. 131–136.

[53] E. Goldstein, A. Apolloni, B. Lewis, J. C. Miller, M. Macauley, S. Eubank, M. Lipsitch, and J. Wallinga, "Distribution of Vaccine/Antivirals and the 'Least Spread Line' in a Stratified Population," *J. R. Soc. Interface*, 2009.

[54] S. Wright, "Primal-Dual Interior-Point Methods." *Siam*. 2006.

[55] Y. Zhou, Z. Ma and F. Brauer, "A Discrete Epidemic Model for SARS Transmission and Control in China," *Math. and Computer Modelling*, 2004, Vol. 40, pp. 1491–1506.

Curriculum Vitae

Paula Andrea Gonzalez Parra was born in Cali-Colombia. The first daughter of Luis Arturo Gonzalez and Maria Isabel Parra, she graduated from Universidad del Valle, Cali, in December of 1996 with a major in mathematics. She got her master in Mathematics in the same university on December of 2002. She was a teaching assistant and a full time lecturer at the Mathematical Science Department in Universidad del Valle from 1996 to 2004. She worked as a full time lecturer at the militar school Marco Fidel Suarez in Cali. In 2005 she got a full time position at the Universidad Autonoma de Occidente.

Paula started the doctoral program in Computational Science at UTEP in 2009. Her advisor, Dr Martine Ceberio, was her professor in advanced algorithms and logical foundation for computer Science. These classes were a big challenge for Paula, but thanks to Dr. Ceberio, who is a great professor and a great mentor, she was able to overcome this challenge and succeeded. Paula met Dr Carlos Castillo-Chavez, her dissertation co-chair, and she has attended the Mathematical and Theoretical Biology Institute MTBI in 2000, 2009-2012.

Paula has been the recipient of honors and awards including an International Fellowship from the American Association from University Women, a Cotton Scholarship from University of Texas at El Paso, and a Scholarship from the Pan American Round Table of Texas. She has presented her research at national and international conferences meetings including SIAM and SACNAS conferences; the Mathematics in Emerging Infectious Disease Management Conference, Cuernavaca, Mexico and Congreso Latinoamericano de Biologia Matematica Armenia, Colombia.

After graduation, Paula will return to her home town Cali, Colombia to continue her career as Professor in Universidad Autonoma de Occidente.

email: paulag817@gmail.com